scientific reports

Check for updates

OPEN

Mechanical and impact behavior of lightweight geopolymer concrete produced by pumice and waste rubber

Ali İhsan Çelik[1], Memduh Karalar[2], Ufuk Tunç[1], Mehmet Fatih Şahan[3], Essam Althaqafi[4], Osman Ahmed Umiye[5,6]✉ & Yasin Onuralp Özkılıç[6,7]✉

The study examined the impact of incorporating pumice and rubber obtained from waste tires as aggregate in specific ratios on geopolymer concrete (GPC). For this aim, various combinations and replacement percentages of pumice and waste tire rubber (WTR) were tested in GPC. Pumice was replaced with coarse aggregate in varying proportions of 0%, 5%, 10%, and 15% and WTR was added into mixture with same proportions. A total of 144 GPC specimens were cast and tested. Tests were performed to measure the compressive strength (CS), splitting tensile strength (STS), flexural strength (FS) and dynamic drop-weight tests. Evaluations of the setting time and workability were also conducted. When natural coarse aggregate was substituted with pumice in concrete, the strength of the resulting mixtures fell. The second research varied the percentage of WTR in the concrete mixture from 0%, 5%, 10%, and 15% while keeping the pumice percentage stable. The study showed that when the pumice ratio was set as constant, there was a steady loss of strength as the percentage of WTR increased. The experimental results demonstrated that partial replacement of coarse aggregate with pumice (up to 15%) led to a progressive reduction in both CS (up to 18.17%) and STS (up to 37.13%) of GPC. This decline in strength became more pronounced with the concomitant utilization of WTR. The findings demonstrated that as the WTR content elevated from 0 to 15%, there was a consistent decline in FS across all levels of pumice replacement, with reductions ranging approximately between 20 and 26%. Additionally, the study created an empirical formula related to STS and CS and compared with the formulas previously developed by various researchers. Scanning electron microscopy (SEM), Energy dispersive x-ray (EDX), and thermal gravimetric analysis (TGA) are also conducted. According to the data gathered from the impact tests, adding pumice to concrete has a negative impact on its impact behavior; on the other hand, adding 10% WTR has a favorable impact.

Keywords Geopolymer concrete, Recycling, Pumice, Rubber, Workability, Setting time, Compressive, Flexural, Splitting, Dynamic drop tests

Abbreviations

GPC	Geopolymer concrete
CS	Compressive strength
STS	Splitting tensile strength
FS	Flexural strength
SEM	Scanning electron microscopy
EDX	Energy dispersive X-ray
TGA	Thermal gravimetric analysis

[1]Department of Construction, Tomarza Mustafa Akincioglu Vocational School, Kayseri University, Kayseri 38940, Turkey. [2]Department of Civil Engineering, Zonguldak Bulent Ecevit University, Zonguldak, Turkey. [3]Department of Civil Engineering, Adıyaman University, Adıyaman, Turkey. [4]Civil Engineering Department, College of Engineering, King Khalid University, 61421 Abha, Saudi Arabia. [5]Department of Civil Engineering, Faculty of Engineering Technolgoy, Zamzam University of Science and Technology, Mogadishu, Somalia. [6]Department of Civil Engineering, Faculty of Engineering, Necmettin Erbakan University, Konya 42000, Turkey. [7]Department of Unique Buildings and Constructions Engineering, Don State Technical University, 344003 Rostov-on-Don, Russia. ✉email: osmanomiye@zust.edu.so; yozkilic@erbakan.edu.tr

FA Fly ash
WTR Waste tire rubber

Granulated volcanic pumice is a naturally occurring lightweight aggregate that resembles a sponge. It is created when molten lava cools quickly. Mediterranean nations, including Greece, Italy, Spain, and Turkey are rich in it[1]. In many countries, it can be employed as an aggregate in the creation of concrete that is lightweight[2]. As gases in the liquid lava particles are retained during cooling, lots of small air spaces or bubbles develop, forming the porous structure of pumice. Because of its lightweight, strong durability against fire, great noise and heat insulation, adequate CS, and acceptable elasticity, as well as a porous composition with low permeability and non-combustibility, pumice is a desirable choice for lightweight aggregate[3]. Over the last ten years, GPC-based structures have garnered a lot of attention despite being relatively new technology in the construction industry.

Geopolymers, which bond like cement and are cheaper and greener than cement, are favored for building applications. The combination of extensive manufacturing, rising landfill costs, limited landfill space, and stricter disposal rules, recycling fly ash (FA) has become a major issue. FA is best used to make GPC by dissolving Si and Al in an alkaline activator and polycondensing to form a firm solid. Therefore, GPC made of FA can be a great alternative to regular cement in meeting the rising demand for concrete as a building material while also reducing the negative impact on the environment caused by the production of regular cement. In terms of the early development of strength, it was discovered that the oven curing technique was the most beneficial and effective approach for curing GPC. Nevertheless, it is challenging to perform this type of curing for applications that are cast in situ.

In recent years, there have been several research studies conducted on the combination of geopolymer material with pumice as a lightweight aggregate due to its popularity and the desired properties of pumice. The characteristics of geopolymer mortars with different mix parameters, both fresh and hardened, were examined by Ekmen et al.[4] Pumice aggregate was used in the production of mortars. Workability, rheology, and mechanical characteristics of the hardened mortars were among the engineering attributes that were being studied. A consistent aggregate mix was calculated to attain acceptable CS and generate lightweight mortar, considering the impact of pumice aggregate on the mechanical characteristics. Top and Vapur[5] developed FA-based GPC by employing a combination of basaltic pumice aggregates and FA (Class F) for the construction of lightweight GPC. It was discovered that the addition of more basaltic pumice aggregate led to a reduction in the material's strength. Kabay et al.[6] evaluated the mechanical, physical, and microstructural properties of geopolymer pastes and mortars made from ground granulated blast furnace slag and pumice, using sodium hydroxide (NaOH), potassium hydroxide, and sodium silicate (Na_2SiO_3) solutions as activators. The test findings demonstrated that the CS of the geopolymer mixes was mostly influenced by the amount of the activator and the proportion of the pumice. Nevertheless, the inclusion of 60%, 70%, and 80% of pumice in the binder did not result in substantial alterations to the mechanical characteristics of the geopolymer mortars. Safari et al.[7] demonstrated that the mixes achieved their highest FS and CS when subjected to oven curing at a temperature of 60 °C for 120 h, using an alkali solution with a concentration of 12 M.

Aly et al.[8] investigated the use of WTR in GPC as a substitute for aggregates. The study presented a rubberized GPC combination that exhibits exceptional strength, ductility, and impact resistance. This mixture was specifically designed for use in structural components that are exposed to dynamic loads and impacts. Upon concluding the investigation, CS of slag-based GPC improved slightly when the crumb rubber fraction was increased to 10%. The possibility of using recycled tire crumb rubber in GPC was established by Park et al.[9] To investigate the impact on the CS of rubberized GPC, various parameters were analyzed. These parameters included the concentration of NaOH solution, the sizes and quantities of aggregates, the curing temperatures and methods, and the duration of curing. The specific effects were observed based on the different types of FA used. The study revealed a negative correlation between the crumb rubber concentration and the CS of GPC. Dong et al.[10] measured the mechanical and durability parameters of rubberized GPC using ten mixes with varying rubber components, binder compositions, and treatment techniques. The results demonstrated a significant relationship between bulk density, elastic modulus, ductility, STS, and water absorption and the CS of rubberized GPC. The study conducted by Pham et al.[11] examined the impact of varying amounts of crumb rubber, which replaced a portion of both the coarse and fine particles in GPC. Investigators conducted tests on three distinct volume proportions, namely 0%, 15%, and 30%. The testing findings demonstrated that rubberized GPC consistently demonstrated superior impact resistance in comparison to conventional GPC, as indicated by the start and progression of cracks, collapse mechanism, and standardized energy absorption. Due to the large pace of production of waste tire rubber (WTR) across the world and the potential for adverse health and environmental effects if they accumulate in the environment and water, the presence of these tires in natural settings is a major cause for concern[12,13]. The environmental impact of employing this ecologically damaging waste material in concrete is lessened, and it is utilized as an innovative construction material to tackle scrap tire concerns.

Dheyaaldin et al.[14] performed another investigation. The purpose of this research is to investigate the advantages of using waste tire aggregate as an alternative to pumice aggregate in alkali-activated slag mortars within the range of 0–60% (by volume) replacement ratios. Furthermore, mortar mixtures were supplemented with silica fume at a concentration of 10% by volume. Use of wasted tire aggregate significantly reduced mechanical strength and durability, according to test results. Significant improvements in mechanical strength and durability, particularly at an early age, have been achieved with the use of silica fume. Although it was noted that the compressive strength (CS) decreased steadily when waste tire aggregate was introduced to the mixture as an aggregate, the mixture that contained 10% silica fume and 0% waste tire aggregate exhibited the highest compressive strength of all the combinations that were examined. The effects of silica fume and WTR aggregates on the characteristics of a lightweight geopolymer composite were studied by Mabrouk et al.[15] at 80 and 100 °C

for curing. To achieve this, WTR aggregates replaced the pumice aggregate in the light geopolymer at varying rates (15%, 30%, and 45% by volume) and silica fume replaced 20% of the ground granulated blast furnace slag. When the amount of WTR aggregates and silica fume was increased, both the CS and flexural strengths (FS) declined, particularly at higher temperatures. When WTR particles and higher curing temperatures were added to lightweight geopolymer composites, their CS reduced. Addition of 20% silica fume resulted in additional reductions of 34.22–187.99%, while CS fell by up to 25.18% at 80 °C and 33.85% at 100 °C.

As previously mentioned, several studies have been conducted in the literature on the effects of concrete containing varying percentages of rubber and pumice particles on GPC[16–19]. The individual impacts of these two products on GPC have been studied independently. However, the lack of research investigating their combined consequences represents a significant gap in existing literature. Furthermore, there is a lack of information in the literature about the response of GPC, including these two materials, when subjected to impact loading. The purpose of this study is to fill in this information gap that has been identified in previous research on this Topic. Consequently, this research provides many significant contributions to existing literature. To accomplish this goal, coarse aggregate was substituted with pumice and waste rubber in different ratios. To do this, it was decided to create 12 mixtures, each with a different ratio of pumice to rubber replacement.

Material and methods

Experimental program

In this study, the coarse aggregate was replaced with 3 different ratios of pumice by weight and WTR was added into mixture by volume ratio. The experiments were carried out in the laboratory department of Construction at Kayseri University. Few research[9,11] have addressed this issue, however those that have used crump rubber by volume percentages of 0%,15%, and 30% have ignored the impact effect. In these studies, it has been stated that there is a decrease in strength values after a certain rate. For this reason, in the mixture, pumice was replaced with coarse aggregate at the rates of 5%, 10% and 15% by weight. Then, tests were carried out with the addition of 5%, 10% and 15% WTR by volume of coarse aggregate.

Materials properties of GPC

The flow chart depicting the mixtures used in GPC concrete production is displayed in Fig. 1. The parameters of this study are distinguished by different colors. The properties of the chemical compounds for a 13 Molar solution of NaOH and Na_2SiO_3 are shown in Table 1. The properties obtained from suppliers are shown, although there are variations depending on factors such as physical state and contaminants.

Lightweight GPC was produced using FA-based geopolymer binder and lightweight aggregate substitutes. The mix design used only FA as the binder, and this binder was activated with an alkali activator consisting of Na_2SiO_3 and NaOH solutions. The total binder/alkali activator ratio was approximately 0.57, and the Na_2SiO_3/NaOH ratio was kept constant at 2.34. To obtain"lightweight"GPC, certain proportions of the coarse aggregate fraction were substituted with pumice. Pumice, thanks to its low density and high porosity, reduced the unit weight of the mix. WTR was used to reduce density and improve energy absorption capacity and impact resistance. As shown in Table 2, the coarse aggregate was substituted with pumice at 5%, 10%, and 15%. Similarly, WTR were added in the same proportions; in some mixtures, pumice and WTR were used together, resulting in a more significant lightness.

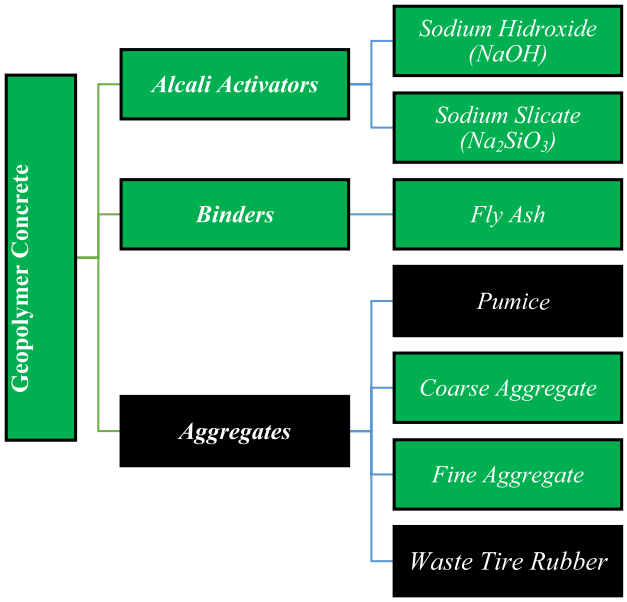


Fig. 1. Flow Chart of GPC production.

Chemical properties	NaOH	Na_2SiO_3
Purity Level	%98–99	–
Molecular Weight	40.00 g/mol	122.06 g/mol
Melting Point	318 °C	–
Boiling Point	1390 °C	1088 °C (for anhydrate form)
Solubility	Very soluble in water	–
Appearance	White and solid as pallet	White and Liquid solution
Odor	Odorless	Odorless
Baumé (20 °C, Bé)	–	48–50
Density (20 °C, g/cm^3)	–	1.50–1.53
SiO_2 (%)	–	28–32
Na_2 (%)	–	13–16

Table 1. Component of NaOH and Na_2SiO_3.

Test No	Set#	S. No #	Fly ash (kg)	Na_2SiO_3 (kg)	NaOH (kg)	Fine aggregate (kg)	Coarse aggregate (kg)	Pumice aggregate (kg)
1	Set#1	GPC_P0_RO	410	164.7	70.3	649.3	1205.7	0.0
		GPC1_P5_R0					1145.4	60.3
2		GPC2_P10_R0					1085.0	120.8
3		GPC3_P15_R0					1024.9	180.9
4	Set#2	GPC4_P5_R5					1145.4	60.3
5		GPC5_P10_R5					1085.0	120.8
6		GPC6_P15_R5					1024.9	180.9
7	Set#3	GPC7_P5_R10					1145.4	60.3
8		GPC8_P10_R10					1085.0	120.8
9		GPC9_P15_R10					1024.9	180.9
10	Set#4	GPC10_P5_R15					1145.4	60.3
11		GPC11_P10_R15					1085.0	120.8
12		GPC12_P15_R15					1024.9	180.9

Table 2. GPC mix materials.



Fig. 2. The utilized pumice and WTR.

The mixing ratios for GPC with pumice replacement and WTR additions are presented in Table 2. The reference GPC mix in the research is represented by the symbol GPC_P0_RO. For instance, the designation GPC1_P5_R0 denotes a mixture of GPC with a pumice concentration of 5% and no WTR. In the same way, GPC5_P10_R5 designates a GPC combination containing 10% pumice and 5% WTR. The utilized pumice and WTR are given in Fig. 2.

This experimental study focuses on the mechanical properties and load-bearing capacity of lightweight GPC. It is known that the strength properties decrease as the proportion of pumice and rubber increases[20]. The optimum partial replacement ratio of coarse aggregate with pumice aggregate in concrete is determined to be 5%, but it can go up to 15%[21]. Based on this, the replacement ratios have been set at 5%, 10%, and 15% as shown in Table 2, to ensure that the CS of the GPC obtained from this experimental study does not decrease significantly. Additionally, for each fixed pumice, WTR was also added with ratio 5%, 10%, and 15% by volume of coarse aggregate.

The binder (FA) and aggregate (fine and coarse aggregate, and pumice) quantities are clearly presented in Table 2 and the binder/aggregate ratio was kept constant. Throughout the study, water was not added to the mix as any additional free water; the required fluidity was achieved through an alkaline activator solution (Na_2SiO_3 + NaOH). Therefore, the "activation solution/binder" ratio was considered instead of the "water/binder" ratio, and this ratio was kept constant for all mixes. Workability parameters were monitored during the pouring of the mix, and no workability problems were encountered while placing the mixes in the mold. However, the binder/aggregate ratio and the effectiveness of the solution used in the mix will be highlighted in the text for clarity. Binder/total aggregate = 410/(649.3 + 1205.7) ≈ 0.23, alkali activator/binder = 235/410 ≈ 0.57 and Na_2SiO_3/NaOH ratio = 164.7/70.3 ≈ 2.34. No free water was added, workability was provided entirely with the activator solution.

For the study, aggregate from WTR was obtained by shredding tires and resizing them to match the coarse aggregate specifications defined within the scope of the study. The pumice aggregate had a diameter ranging from 6 to 11 mm. Additionally, the chemical composition of both the FA[22] and pumice aggregate was detailed in Table 3.

First of all, 40 mm × 40 mm × 160 mm prism-shaped samples were prepared in accordance with ASTM 349[23] Standard for FS. After FS, cube samples with dimensions of 40 mm × 40 mm × 40 mm were used in CS[24]. The use of smaller specimens, such as 40 mm × 40 mm × 40 mm cubic blocks, for the CS test was chosen to ensure the economical use of resources. Additionally, cylindrical samples with dimensions of 100 mm in diameter and 200 mm in height were prepared in accordance with the ASTM C496/C496M[25] for splitting tensile strength (STS). A laboratory concrete mixer was used to achieve a homogeneous mixture, and the mixture was poured into molds. The process of placing GPC into molds involved detailed compression and vibration procedures. In the reference mixture used in the study (P0–R0), slump values were observed to be in the range of approximately 70–100 mm, and workability lasted 25–35 min. As pumice replacement increased, slump values decreased significantly. At P15, slump decreased to 35–55 mm, while workability duration remained unchanged. WTR addition, on the other hand, had a more limited effect, decreasing slump by 5–15%, while workability time remained in the range of 25–40 min. In mixtures where pumice and WTR were used together, the effects were cumulative, with slumps decreasing to 30–50 mm and workability time remaining between 20–30 min. These values are within reasonable ranges depending on the material properties used and are consistent with the fresh mix behavior observed in the study. The samples underwent a curing process in an oven at 85 °C for 24 h. Curing at 85 °C for 24 h accelerates the chemical reaction rate of geopolymer concrete (GPC), leading to early strength gain. Additionally, this temperature enhances the microstructural strengthening of the concrete, contributing to the improvement of its mechanical properties[26,27]. The samples were kept in a laboratory environment with an average temperature of 21 °C and a humidity level of 35% for 28 days after oven curing. To evaluate the performance of GPC incorporating pumice and WTR, five different types of experiments were conducted. Additionally, dynamic drop-weight tests were carried out as an impact test. Each of these tests was carried out in triplicate for every combination and type of test. The preparation, compaction, and curing processes for the test samples are depicted in Fig. 3.

Component	Fly ash%	Pumice %
SiO_2,a	57.3	63.37
Al_2O_3,b	24.9	17.90
Fe_2O_3,c	7.24	2.80
CaO	3.98	8.351
SO_3	0.47	0.075
Na_2O	1.35	3.74
K_2O	2.19	2.2
Cl^-	0.05	–
MnO	–	–
K_2O	–	1.195
TiO_2	–	0.144
NiO	–	0.007
SrO	–	–
ZrO2	–	0.013
Sludge (> 45 µm)	2.52	0.21

Table 3. Component of FA and pumice.



Fig. 3. Sample preparation.



Fig. 4. Testing procedures and post-failure views of the specimens.

GPC gains its necessary strength and durability through the oven curing process, which activates chemical components such as alumina and silicate. The oven curing of GPC should be conducted swiftly and under controlled conditions. The specific application process and conditions can vary based on the concrete mix used, its intended application, and the requirements. These samples were removed after curing in the oven for 24 h at 85° and stored outdoors for 28 days to undergo testing. The FS, CS, and STS tests, conducted in accordance with the relevant standards, are presented in Fig. 4. In addition, post-test images of the fractured specimens are included to provide visual insight into the failure modes and damage characteristics.

Dynamic drop-weight tests

A specific weight is dropped on the sample from a predetermined height to conduct a drop-weight impact test. Drop-weight tests come in two varieties: instrument-free and instrument-equipped. The dynamic properties of the material are ascertained using the instrumented drop-weight impact test method. In contrast to other approaches, the instrumented impact test system can execute the sample's sticking, puncture, and repeated impact tests by modifying different heights and weights to produce the necessary energy[22,28,29]. In comparison to other tests, the dynamic drop-weight test stands out as a very advantageous option, especially with respect to fracture development and propagation. The ability to evaluate how the fracture spreads and how much energy the material being examined is able to absorb in the event of a rapid impact is made possible by this. In comparison to traditional mechanical testing, it replicates loading situations that are more rapid. The setup details for the drop-weight test are displayed in Fig. 5. A total impact load of 16.235 kg consisting of the loading frame, striking tip, and additional mass was dropped on the cylinder specimen, which was standing upright at the bottom of the chamber, from a height of 314 mm. The energy impact was 50 Joules. The impact load was transferred to the specimen using an impact strain gauge tube with a 63.5 mm diameter hemispherical striking tip. The data in the impact strain gauge tube was collected with the help of a data collector, and force–time and energy-time graphs were obtained.



Fig. 5. Instrumented drop-weight test machine.

Experimental consequences and discussions

The primary objective of this research project is to conduct a comprehensive evaluation of various production-based sub-assemblies of GPC with additions of pumice and WTR. To accomplish this objective, the coarse aggregate was substituted with three varying proportions of pumice and WTR tires. In addition to the reference, the pumice in the mixture was switched out for coarse aggregate at the percentages of 5%, 10%, and 15% respectively. After that, experiments were performed with 5%, 10% and 15% of WTR added to the mixture. Following the completion of the analysis, the CS test, STS test, and FS test were carried out. Moreover, SEM, EDX, and thermal gravimetric examination were also accomplished. The results of the examination will be discussed in the sections that follow.

Comprehensive investigation of the compressive test (CS)

The impact of pumice on the CS

This section of the study aims to provide a thorough assessment of several production-based sub-assemblies of pumice-added GPC. An assessment was conducted to determine the impact of partially replacing the aggregate in concrete with pumice on the CS of cube specimens. To achieve this goal, the concrete's PR was adjusted to 0%, 5%, 10%, and 15% in Set#1. Pumice was used to replace natural coarse aggregate in concrete, and the results showed that the CS of the concrete decreased by 2.5%, 5.64%, and 13.25%, respectively, with replacement rates of 5, 10, and 15%.

As observed in Set #2, a pumice ranging from 0 to 15%, along with 5% WTR, was added to the mixture. This resulted in a mean CS of 34.41 MPa for a replacement ratio of 5%. Additionally, the average CS values for replacement ratios of 10% and 15% were 33.12 MPa and 29.92 MPa, respectively, reflecting reductions in CS of 3.74% and 13.05%, respectively, compared to the control concrete. In Set #3, a pumice varying from 0 to 15%, along with 10% WTR, was incorporated into the mixture. For a replacement ratio of 5%, this resulted in a mean CS of 32.18 MPa. Additionally, the mean CS values for substitution rates of 10% and 15% were 31.11 MPa and 29.22 MPa, respectively.

Based on the data provided, the concretes'respective CS decreased by 3.32% and 9.19%. In the final trials, as shown in Set #4, a pumice ranging from 0 to 15%, along with 15% WTR, was added to the mixture. This resulted in an average CS of 28.46 MPa for a replacement ratio of 5%. The average CS values for 10% and 15% replacement ratios were 26.36 MPa and 23.34 MPa, respectively, reflecting decreases of 7.37% and 18.17%. The test results indicated that altering the pumice from 0 to 15%, in combination with the addition of WTR, has an inverse effect on the mixture's CS, as shown in Fig. 6.

The outcomes are comparable to those reported in the literature. Oz et al.[30] investigated the effect of common pumice on the workability of self-compacting concrete. The researchers concluded that as the pumice content increased, the CS of the concrete decreased. This reduction in CS was observed with the increased proportion of pumice in the mixture. The discrepancy arises because the specific gravity of pumice is significantly lower than that of crushed stone, leading to reduced strength when compared to mixtures containing crushed stone[30]. In Shafiq et al.'s study[31], the CS of concretes containing pumice was compared to the CS of concretes that were traditionally made with natural aggregate at different curing times. According to the test findings, there

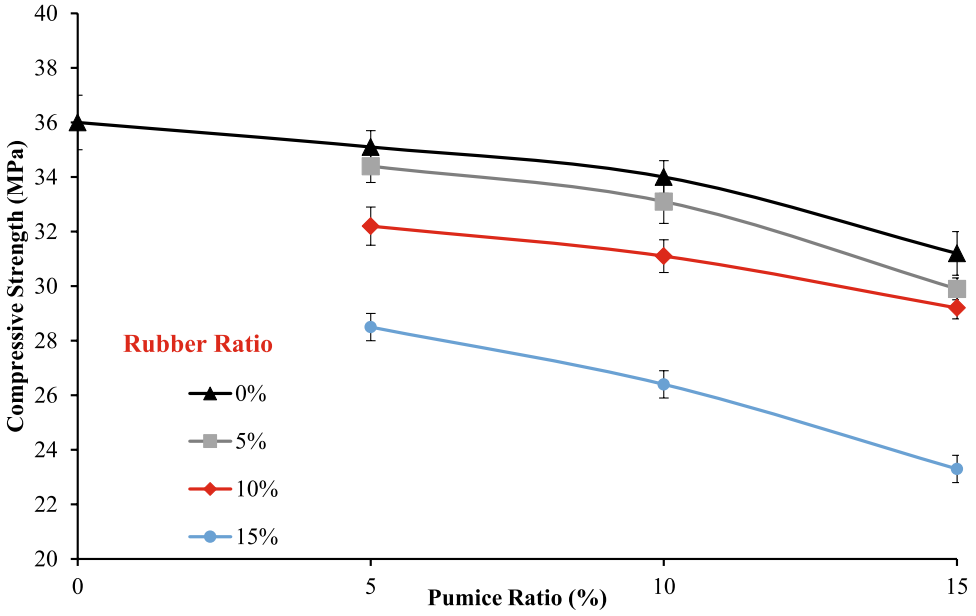


Fig. 6. Compressive test results.

was a strength reduction of around 1%, 26%, 37%, and 50% when natural aggregate was partially substituted with pumice. According to the findings of Parhizkar et al.'s study[32], the CS reduced as the amount of pumice replacement increased. To build a structural lightweight concrete, a laboratory study using FA as a mineral additive and basaltic pumice as the aggregate was partially examined by Yasar et al.[33] Two types of lightweight concrete mixtures were prepared: a control combination consisting of lightweight basaltic pumice and regular Portland cement, and a FA lightweight concrete mixture that replaces 20% of the cement with FA on a weight basis.

Kurt et al.[34]. reported that the CS decreases as the proportion of pumice increases while substituting natural aggregate with pumice in ratios ranging from 0 to 10% with 20% increments. The effects of substituting natural fine and coarse aggregate with pumice aggregate on the CS were examined by Bhavana and Rambabu[35]. The findings indicated a 9.60% drop in CS when 10% of the pumice and fine aggregate were substituted, a 15.13% reduction when 20% was substituted, and a 16.97% reduction with a 30% substitution. Similarly, reductions of 13.28%, 22.51%, and 33.65% in CS were observed when coarse aggregate was substituted. Widodo et al.[36] demonstrated that an increasing volumetric proportion of pumice used as coarse aggregate in concrete causes a systematic decline in the concrete's CS.

It was found that the volume percentage of pumice aggregate, used as coarse aggregate in the mixes, tends to lower the CS in an inversely proportional manner. Kılıç et al.[37]. observed a 72.76% loss in CS when pumice completely replaced natural aggregate. Similarly, Rajeswari and George[38]reported a 65.29% reduction in CS when 70% of the coarse aggregate was substituted with pumice. Desai et al.[39] conducted an experimental study on concretes with pumice replacing coarse aggregate at varying levels, from 0 to 100%. The study revealed a systematic decline in CS as pumice content increased, with reductions of 16.80%, 45.76%, 60.76%, and 68.67% for pumice replacement levels of 25%, 50%, 75%, and 100%, respectively, compared to reference concrete. In a similar investigation, Sultan et al.[40]. progressively replaced coarse aggregate with pumice in 25% increments, ranging from 0 to 100%. Their findings showed that the CS dropped from 27.46 MPa to 14.72 MPa with a 25% replacement, and further declined to 14.01 MPa, 11.74 MPa, and 10.64 MPa for replacement levels of 50%, 75%, and 100%, respectively.

The impact of the WTR ratio on the CS

This part of the research examined the impact of WTR on CS by varying the ratio of rubber while keeping the pumice constant. To achieve this, the proportion of WTR in the concrete mixture was adjusted to 0%, 5%, 10%, and 15%, while the pumice was fixed at 5%. The average CS values for replacement ratios of 0%, 5%, 10%, and 15% were 35.1 MPa, 34.41 MPa, 32.18 MPa, and 28.46 MPa, respectively. It was determined that with a pumice content of 5%, the CS decreased by 1.97%, 8.32%, and 18.92% as the WTR content increased. In a second observation, the pumice was set at 10%, and the percentage of WTR was varied between 0%, 5%, 10%, and 15%. The mean CS values for these replacement ratios were 33.97 MPa, 33.12 MPa, 31.11 MPa, and 26.36 MPa, respectively. The study demonstrated that increasing the WTR content by 5%, 10%, and 15% resulted in CS reductions of 2.50%, 8.42%, and 22.40%, respectively, compared to reference concrete with 10% pumice.

Lastly, the WTR proportion was adjusted from 0 to 15%, while the pumice was fixed at 15%. The average CS values for replacement ratios of 0%, 5%, 10%, and 15% were 31.23 MPa, 29.92 MPa, 29.22 MPa, and 23.34 MPa, respectively. The study showed that increasing the WTR content by 4.19%, 6.44%, and 25.26% led to a gradual decrease in CS compared to the reference concrete containing 15% pumice. The results indicate that the CS

of the concrete is inversely impacted by the variation in WTR content (0–15%) when the pumice is fixed, as illustrated in Fig. 7. These findings align with the literature, where it has been observed that WTR deforms more than the binder under load due to its flexibility. This variation in deformation creates an incompatibility, resulting in microcracks at the rubber-binder interface[41]. Another explanation found in the literature is that the rubber-binder interface dries out as the mixing water used for cement hydration is consumed over time. Since WTR has a weaker bond with the binder compared to aggregate and a higher shrinkage potential, microcracks may form around the rubber particles, acting as points of stress concentration and crack propagation[41].

Detailed examination of the STS

The impact of pumice on the STS

As a result of replacing natural coarse aggregate with pumice in concrete, the results demonstrated a decrease in STS of 3.30%, 16.06%, and 20.66% at 5, 10%, and 15% replacement rates, correspondingly. The research results indicate that an increase in the **pumice** led to a decrease in the STS of the concrete samples. As shown in Set #2, by adding 5% WTR and the **pumice**, which varies from 0 to 15%, to the mixture. With a replacement ratio of 5%, this produced a mean STS of 3.42 MPa. Also noteworthy are the average STS values of 3.02 MPa and 2.88 MPa, respectively, for replacement ratios of 10% and 15%. The data presented indicates that the concretes'STS decreased by 11.68% and 15.93%, respectively. The combination in Set #3 used the **pumice**, which ranged from 0 to 15%, together with 10% WTR to accomplish this objective. A mean STS of 3.19 MPa resulted from using a replacement ratio of 5%. It is also important to note that the mean STS values for 10% and 15% replacement rates are 2.55 MPa and 2.21 MPa, respectively.

The data supplied indicates that the respective STS of the concrete fell by 19.97% and 30.91%. In the last experiments, this was accomplished by adding 15% WTR and a **pumice** that ranges from 0 to 15% to the mixture, as indicated in Set #4. The replacement percentage was 5% and the average STS was 3.02 MPa as a result. Additionally, it is noteworthy to mention the mean STS of 1.90 MPa and 2.22 MPa for 10% and 15% replacement percentages, respectively. According to the findings, there was a 26.61% and 37.13% drop in the concretes'STS. Based on the test results, the addition of WTR to the mixture has an inverse effect on the STS when the **pumice** is changed from 0 to 15%, as demonstrated in Fig. 8. Similar findings to those reported in the literature were found. The impact of substituting pumice for coarse aggregate in concrete samples measuring 100 mm in diameter by 200 mm in length was examined by Manoj et al.[42] It was observed that in comparison to control concrete, the STS dropped at all replacement levels, according to the research's conclusions. To study the STS of concretes, Reddy et al.[43] substituted Pumice in ratios of 25%, 50%, 75%, and 100% for natural aggregate at 28 days. When the replacement level reached 25%, the strength decreased by around 33%. Sangeetha et al.[44] conducted an experimental study to compare ordinary concrete with concrete that had varying percentages (10%, 20%, 30%, 40%, 50%, 60%, 80%, 100%) of pumice replacing the coarse particles. The test findings demonstrated a consistent decline in the STS performance as the pumice content increased.

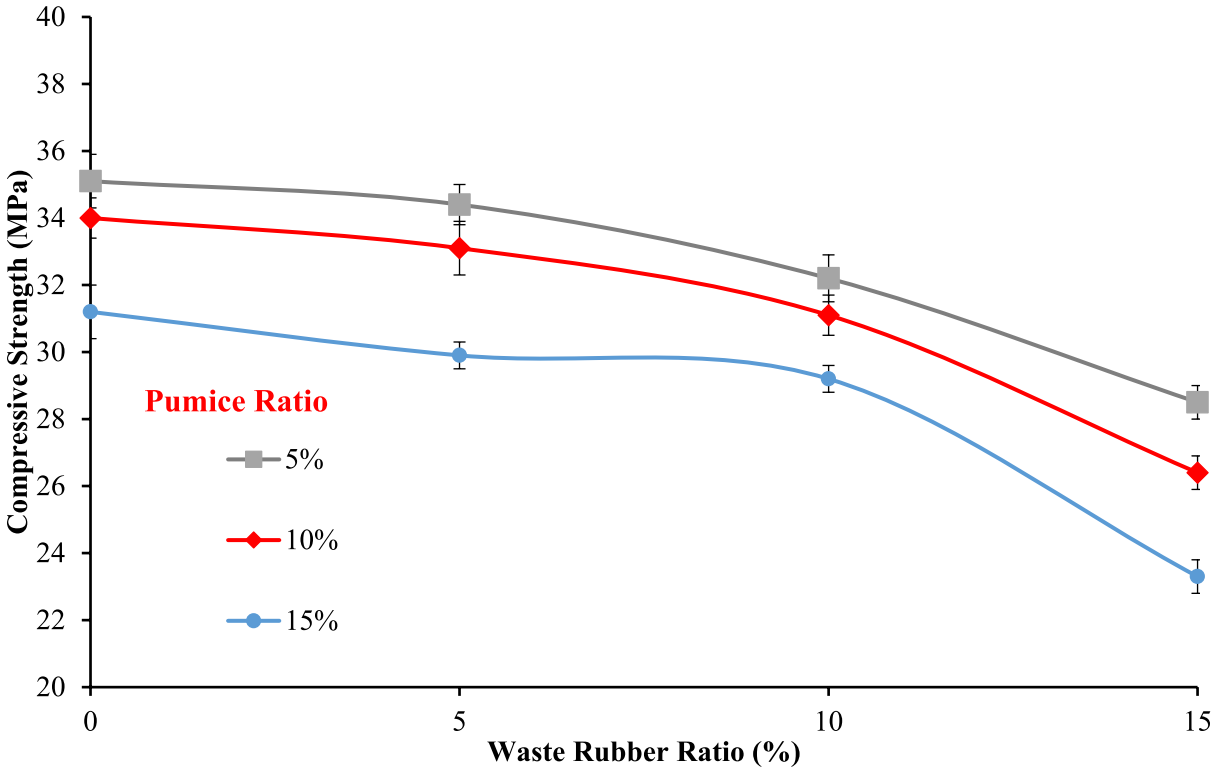


Fig. 7. Compressive test results.

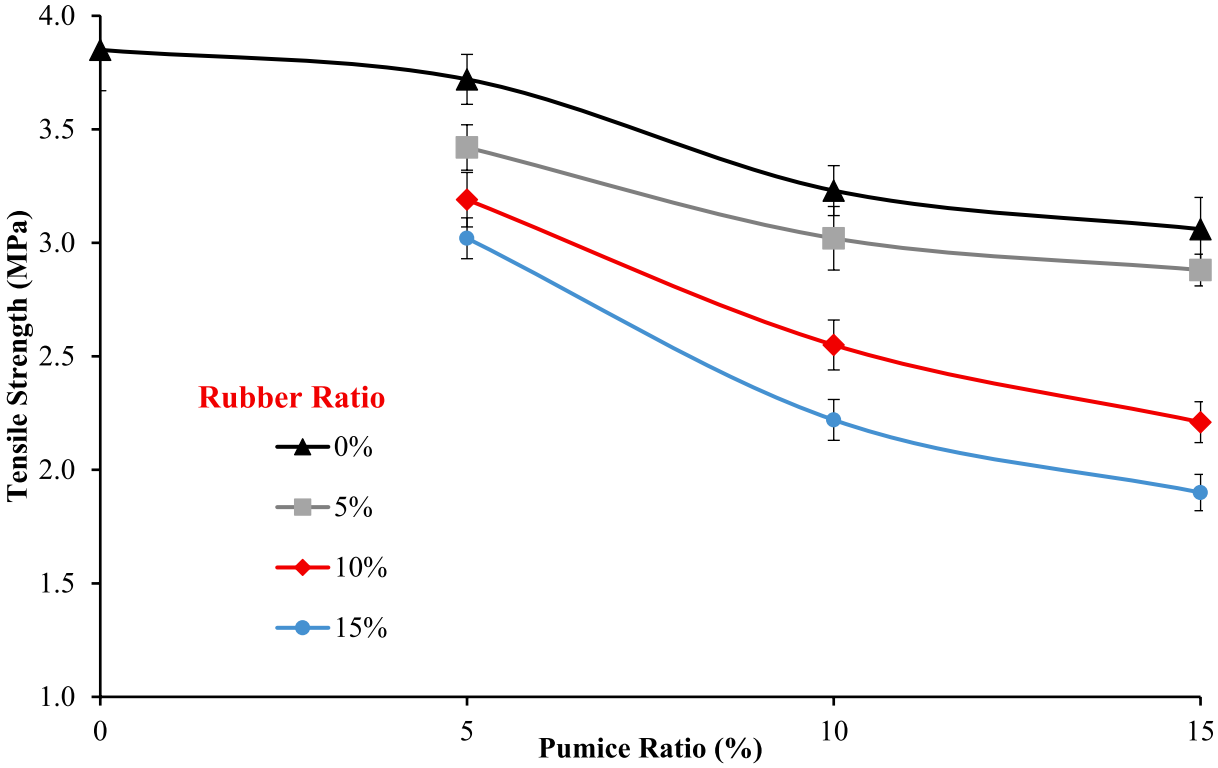


Fig. 8. STS tests.

The impact of the WTR ratio on the STS

This section of the study fixed pumice while adjusting the material proportion to investigate the effect of WTR on STS. To achieve this goal, the pumice was set at 5% and the amount of WTR was changed to 0%, 5%, 10%, and 15% of the concrete mixture, respectively. Remarkably, the average STS measurements for the proportions at 0%, 5%, 10%, and 15% are 3.72 MPa, 3.42 MPa, 3.19 MPa, and 3.02 MPa, respectively. After comparing the reference concrete with pumice at 5%, it was found that the expansion of the WTR ratio content by 8.06%, 14.25%, and 18.82% would lead to a progressive drop in STS. The amount of WTR in the concrete mixture was changed between 0%, 5%, 10%, and 15% in the second investigation, in addition to maintaining the pumice at 10%. It is noteworthy to observe that the average STS values for replacing ratios of 0%, 5%, 10%, and 15% are 3.23 MPa, 3.02 MPa, 2.55 MPa, and 2.22 MPa, in that order. The study showed that when the amount of WTR was increased by 6.50%, 21.05%, and 31.27%, there was a gradual decrease in STS compared to the reference concrete, which included 10% pumice. In summary, the amount of WTR included in the concrete combination varied between 0 and 15%, while the Pumice percentage remained constant at 15%. It is noteworthy to consider the average STS values of 3.06 MPa, 2.88 MPa, 2.21 MPa, and 1.90 MPa, respectively, for the percentages that are replaced by 0%, 5%, 10%, and 15%. The research showed that using WTR at proportions of 5.88%, 27.78%, and 37.91% resulted in a progressive reduction in STS as compared to the reference concrete containing 15% pumice. Test results were given in Fig. 9. These findings show that WTR negatively affects the tensile strength of concrete, and this effect varies depending on the amount of pumice used. In other words, the higher the pumice content, the greater the negative impact of WTR on the concrete. The results of the study concluded that although scrap rubber has potential benefits for sustainability in concrete, it may reduce mechanical performance.

Dynamic drop-weight test results

The force history recorded during the impact tests of the cylinder specimens is presented in graphs. The graphs show the effect of both pumice addition and WTR addition on the impact behavior of the specimens[28]. The values shown are the average values of 3-cylinder specimens from each concrete mix. The force history of the specimens with WTR kept constant and pumice added is given in Fig. 10, 11 and 12. The force–time graphs of the specimens produced with 5% WTR are given in Fig. 10, while the force–time graphs of the specimens produced with 10% WTR are given in Fig. 11 and 15% WTR are given in Fig. 12. As a result of the evaluation of the impact force curves (Figs. 10, 11 and 12) of the specimens in which the pumice was kept constant and the WTR ratio was changed to 5%, 10% and 15% respectively, it was revealed that increasing the WTR ratio caused a decrease in the peak impact force values. This trend was the same for all levels of pumice. The impact force curves of the specimens with different WTR ratios were similar at the beginning but diverged as they approached the peak value. In the unloading region after the peak value, the curves moved further away from each other and approached the zero line in different ways. In the mixtures containing 5% WTR, the specimens containing 5% pumice absorbed energy in the unloading zone in a shorter time, while the specimens containing 10% and

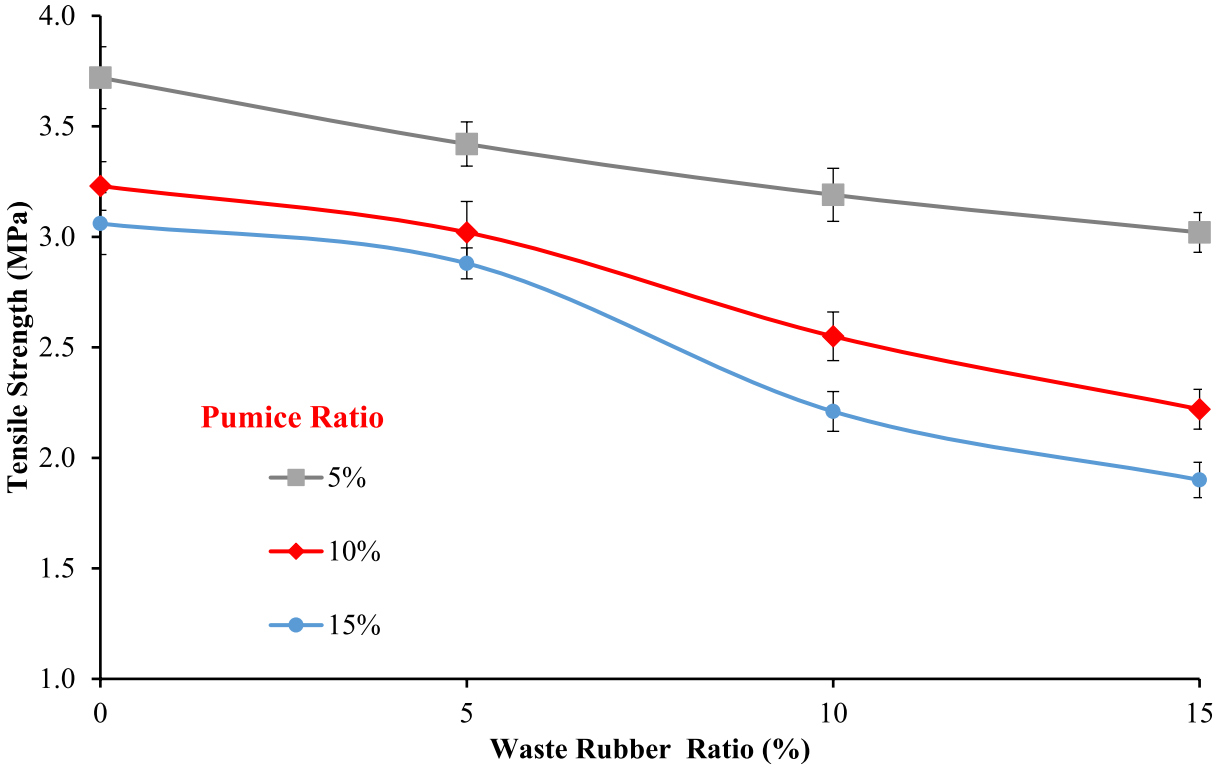


Fig. 9. STS tests.

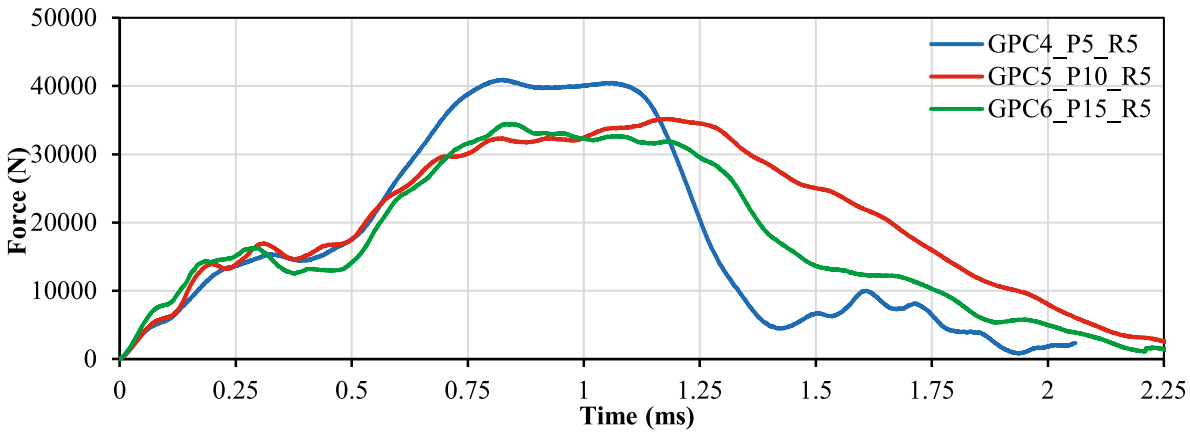


Fig. 10. Average force history of cylinder samples with %5 WTR.

15% pumice absorbed energy in a longer time than the specimens containing 5% pumice. Similar trends were observed in the specimens of the mixtures containing 10% and 15% WTR. The Force history of the specimens to which rubber was added while keeping the pumice constant is given in Figs. 13, 14 and 15. The force–time graphs of the specimens produced with 5% Pumice are given in Fig. 13, while the force–time graphs of the specimens produced with 10% Pumice are given in Figs. 14 and 15% pumice are given in Fig. 15. In mixtures where the pumice was kept constant, the peak impact force increased when the rubber ratio was increased from 5 to 10%, while the peak impact force decreased when the rubber ratio was increased from 10 to 15%. In the force–time graphs where pumice is constant, the mixtures with 10% WTR addition give better results than the others.

The force–displacement graphs obtained from the impact test of the specimens are shown in Fig. 16. In all mixtures, the largest force was 41,168 N in the mixture with 5% Pumice and 10% WTR, while the smallest force was 31,624 N in the mixture with 15% Pumice and 15% WTR. As can be seen from the force–displacement graphs, the 5% Pumice and 10% WTR mixture stood out from the others with the largest reaction and the least

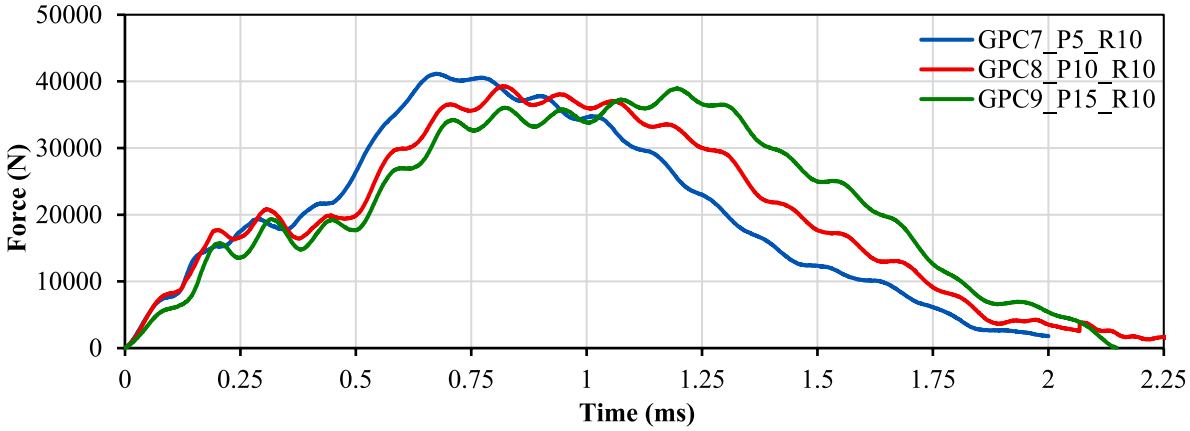


Fig. 11. Average force history of cylinder samples with %10 WTR.

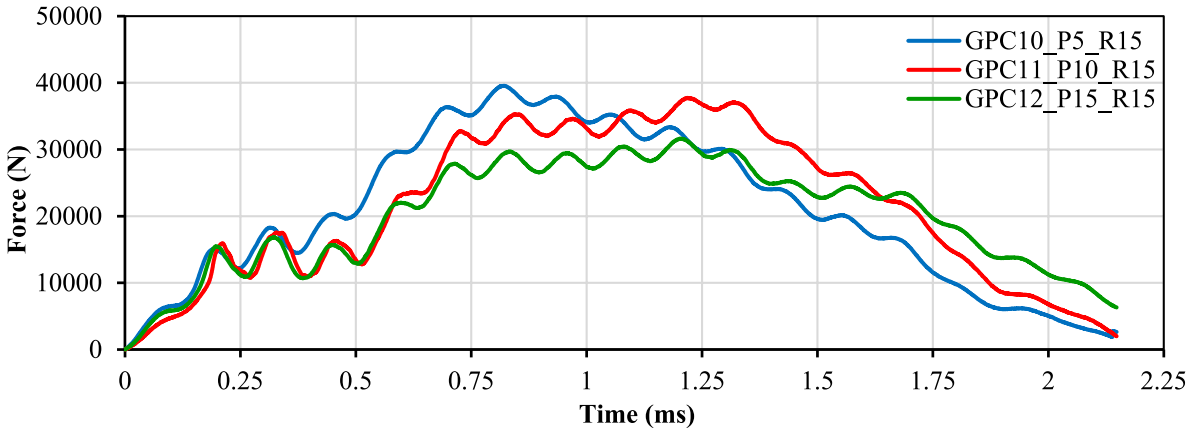


Fig. 12. Average force history of cylinder samples with %15 WTR.

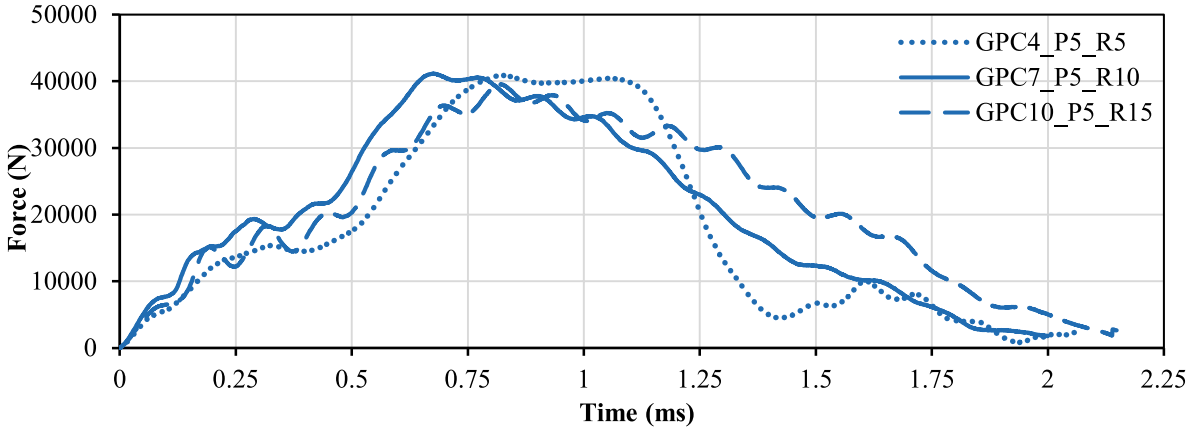


Fig. 13. Average force history of cylinder samples with %5 pumice.

displacement. The best impact performance occurred in concrete specimens with 5% Pumice and 10% WTR mixture.

The damage of some specimens after the impact test is given in Fig. 17. At the given energy level, only cracks were formed in the specimens, and there was no fragmentation in the specimens. Considering the damage to the specimens, some specimens developed cracks while others did not. There is no general trend in the damage of the specimens subjected to impact.

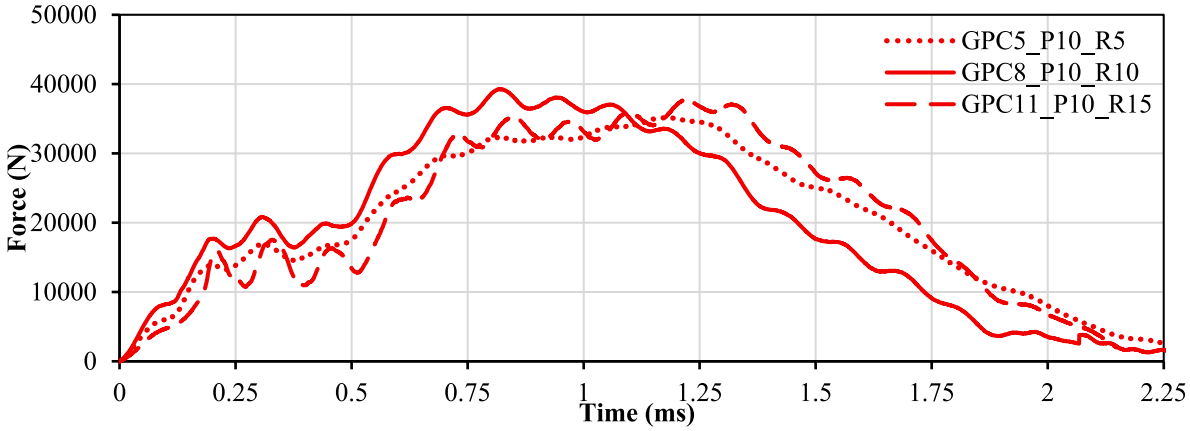


Fig. 14. Average force history of cylinder samples with %10 pumice.

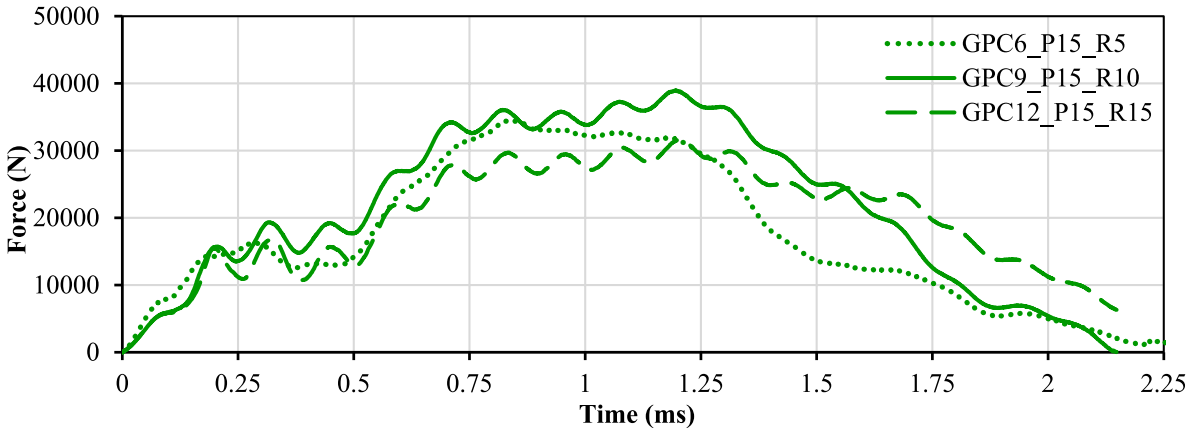


Fig. 15. Average force history of cylinder samples with %15 pumice.

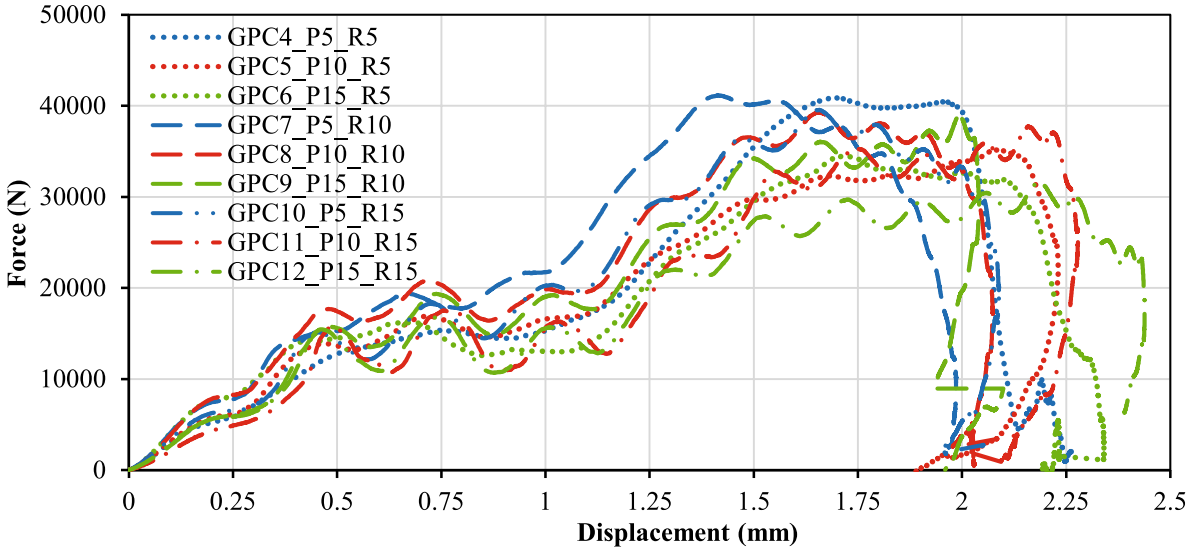


Fig. 16. Average force–displacement history of cylinder samples with %15 pumice.

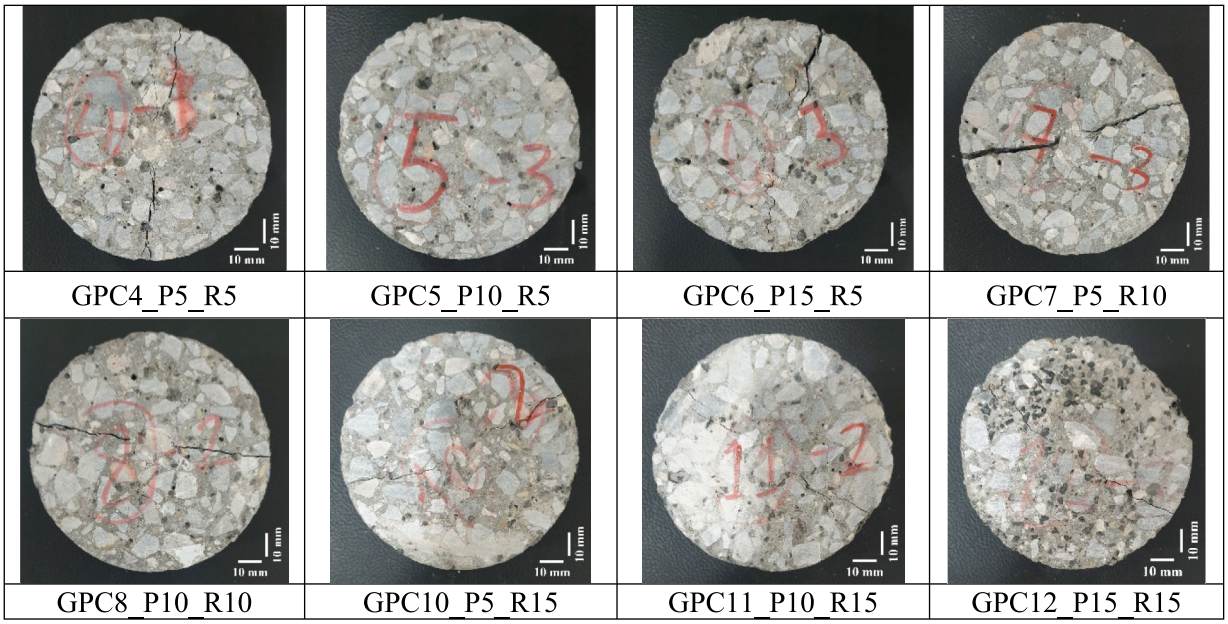


Fig. 17. Damage of some specimens after the dynamic drop-weight test.

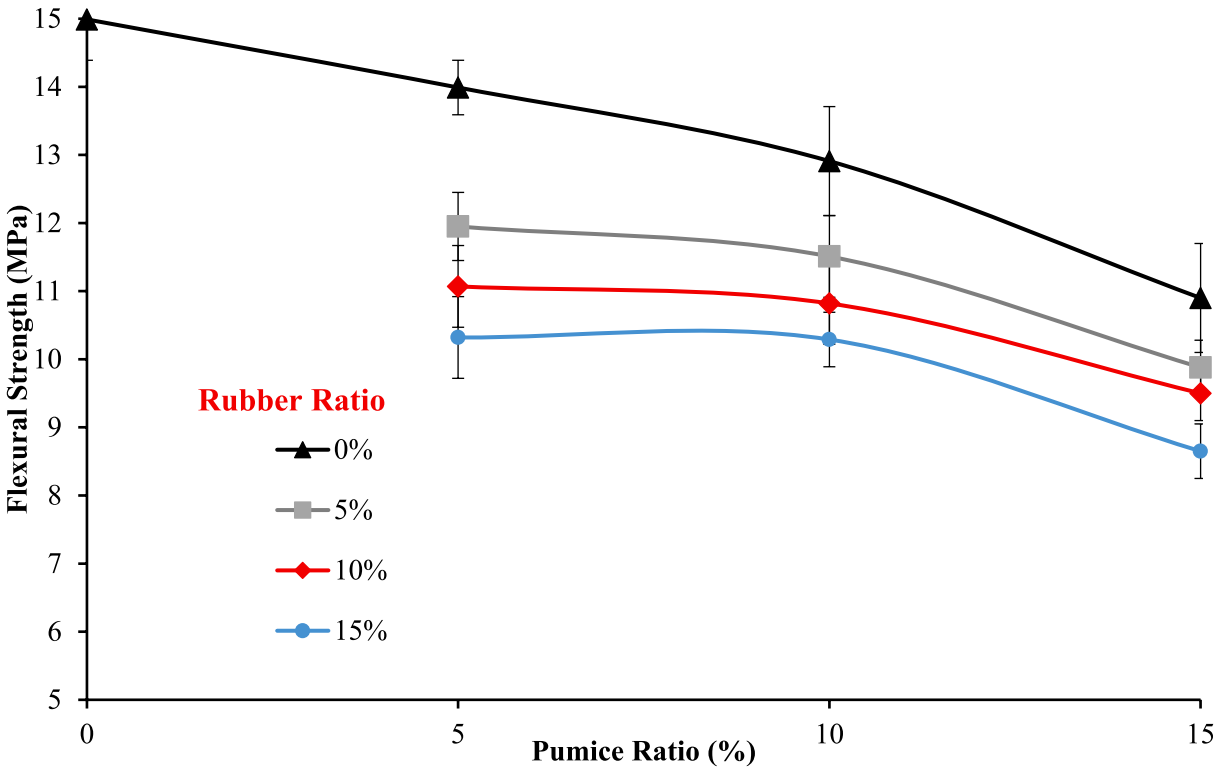


Fig.18. FS test consequences.

Detailed examination of the FS

The impact of pumice on the FS

The replacement of pumice has been demonstrated to result in a reduction in FS, according to the results obtained. Following the data shown in Fig. 18, the control sample has attained a FS of 14.93 MPa after 28 days. As was mentioned before, the pumice of the concrete in Set #1 was altered to one of the following values: 0%, 5%, 10%, and 15%. A replacement ratio of 5% was used, and the mean FS obtained was 13.99 MPa. To add to this, the typical FS value for a 10% substitution proportion was 12.91 MPa, while the value for a 15% substitution

proportion was 10.89 MPa. Since pumice was used instead of natural coarse aggregate in concretes, the findings indicated that the FS decreased by 6.67%, 13.90%, and 27.32% at replacement rates of 5%, 10%, and 15%, respectively. According to the findings of the study, a reduction in the FS of the concrete samples was brought about by an increase in the proportion of pumice inside the concrete. Examining the impacts of WTR was the purpose of the other experiments that were used. To do this, as realized in Set #2, the mixture was supplemented with 5% WTR and the pumice, which ranges from 0 to 15%. The average FS that was created because of this was 11.95 MPa, and the proportion of replacement was 5%. Furthermore, it should be noted that the average FS values for replacement fractions of 10% and 15% are 11.51 MPa and 9.88 MPa, respectively. Based on the data that was provided, it can be demonstrated that the FS of the concretes reduced by 3.68% and 17.29% respectively. Utilizing the pumice, which varied from 0 to 15%, in conjunction with 10% WTR, the combination in Set #3 was able to successfully achieve this goal. When a replacement percentage of 5% was used, the result was a mean FS of 11.06 MPa. For the 10% and 15% replacement rates, the mean FS values are 10.82 MPa and 9.5 MPa, respectively. This is a crucial fact to keep in consideration. According to the information that was provided, the FS of concrete had a decrease of 2.23% and 14.16% respectively. To achieve this goal in the most recent trials, 15% WTR and a pumice that varies from 0 to 15% were added to the mixture. The results of these studies are shown in Set #4. It was determined that the replacement percentage was 5%, and consequently, the average CS was 10.32 MPa. The mean FS for 10% and 15% replacement percentages, respectively, is 10.28 MPa and 8.65 MPa. In accordance with the results, the FS of the concretes had a decrease of 0.32% and 16.15% respectively. According to the findings of the tests, the incorporation of WTR into the mixture has an impact that is opposite to the FS when the quantity of pumice is altered from 0 to 15%, as shown in Fig. 18.

The impact of the WTR ratio on the FS

In this part of the research, the percentage of pumice was constant, but the proportion of material was adjusted to explore the impact that WTR had on FS. To reach this objective, the proportion of pumice to concrete mixture was adjusted to 5%, and the percentage of WTR was varied to 0%, 5%, 10%, and 15%, respectively. Notably, the average FS values for the replacement percentages at 0%, 5%, 10%, and 15% are, in that order, 13.99 MPa, 11.95 MPa, 11.07 MPa, and 10.32 MPa. An increasing decrease in FS would result from expanding the WTR ratio content by 14.60, 20.91, and 26.25%, according to a comparison of the reference concrete with pumice at 5%. In the second investigation, the percentage of WTR in the concrete mixture was varied at 0%, 5%, 10%, and 15%, while keeping the PR constant at 10%. Remarkably, the average FS values for replacement ratios of 0%, 5%, 10%, and 15% are, respectively, 12.91 MPa, 11.51 MPa, 10.82 MPa, and 10.29 MPa. In comparison to the reference concrete, which included 10% pumice, the research demonstrated a progressive reduction in FS when the proportion of WTR was Raised by 10.84%, 16.19%, and 20.32%. In conclusion, the proportion of pumice in the concrete mixture stayed at 15%, while the quantity of WTR added varied between 0 and 15%. Notably, for the replacement proportions of 0%, 5%, 10%, and 15%, the average FS ratios are 10.90 MPa, 9.88 MPa, 9.50 MPa, and 8.65 MPa, respectively. In comparison to the reference concrete that included 15% pumice, the investigation revealed that using WTR at proportions of 9.30%, 12.82%, and 20.59% led to a gradual decrease in FS. Figure 19 displays the test findings.

Prediction of the splitting tensile strength of the GPC

A typical word that may be used to express an empirical formula that was produced by several investigators and exists among STS (f_{spt}) and CS (f'_c) is as follows:

$$f_{t=}k.\sqrt[n]{f_c} \tag{1}$$

While n and k are the constant coefficients, f'_c represents the CS of a concrete cylinder measured in the SI unit. For the experimentally determined constants k and n, the multiple values that have been offered by many investigators and by a variety of concrete design codes are shown here. A study was conducted by Ryu et al.[39] to investigate the connection between the CS and the STS of FA-based GPC and Na_2SiO_3, respectively. Ryu et al.[45] proposed Eq. (2). A correlation among the CS and STS of GPC was obtained by Gunasekera et al.[46] via the application of low calcium FA in the production of GPC. This relationship can be observed in Eq. (3). Another equation was offered by Zaetang et al.[47] as shown in Eq. (4). De Larrard et al.[48] came up with an additional equation, which was suggested in Eq. (5). Lavanya and Jegan[49] offered another equation developed based on 28 days of experimental data regression analysis as shown in Eq. (6). Another investigation was performed by Ramujee and Potharaju[50]. It was determined using regression model analysis that the relationship between the CS and STS of GPC is comparable to that of ordinary Portland cement concrete. Furthermore, it was observed through this research that the ACI-318-99 resemble is suitable for the prediction of the STS of GPC as shown in Eq. (7). Rai et al.[51] and De Larrard and Malier[52] proposed other equations as proposed in Eqs. (8) and (9).

$$f_t = 0.17(f_c)^{0.75} \tag{2}$$

$$f_t = 0.45(f_c)^{0.5} \tag{3}$$

$$f_t = 0.179(f_c)^{0.85} \tag{4}$$

$$f_t = 0.313(f_c)^{0.67} \tag{5}$$

$$f_t = 0.249(f_c)^{0.772} \tag{6}$$

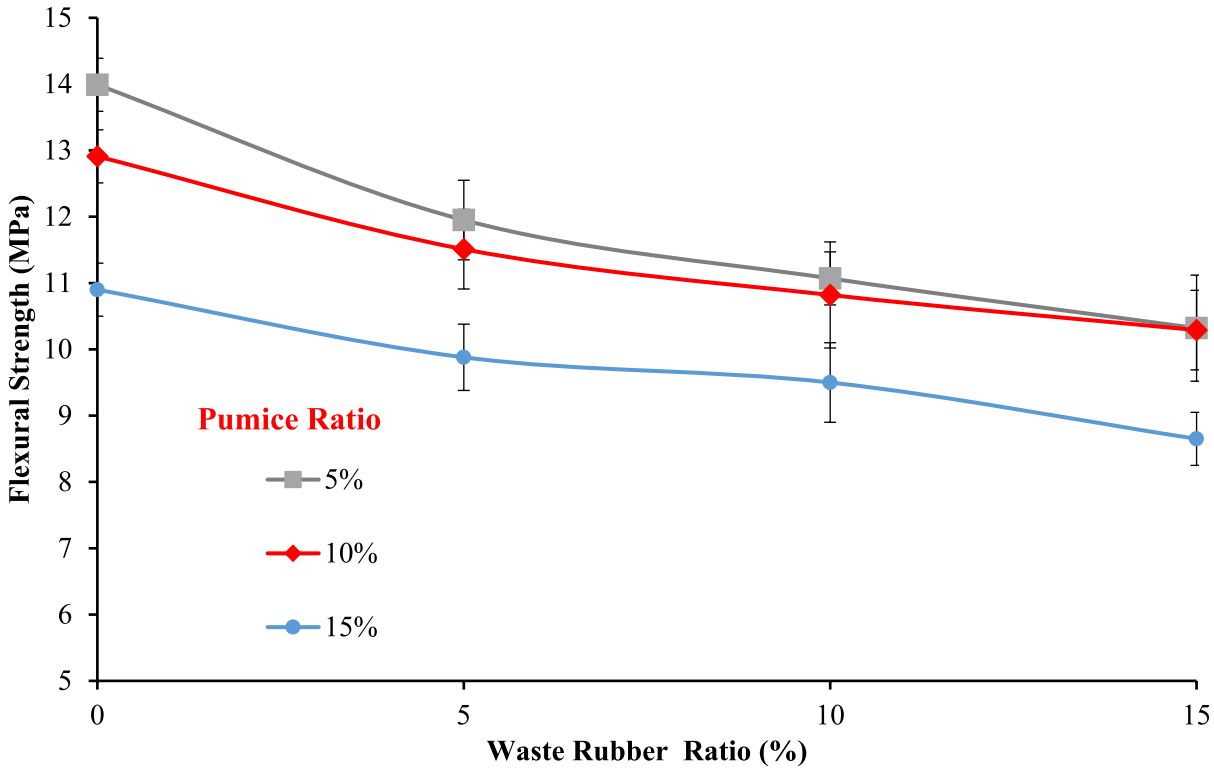


Fig. 19. FS test consequences.

$$f_t = 0.08(f_c)^{0.92} \tag{7}$$

$$f_t = 0.633(f_c)^{0.466} \tag{8}$$

$$f_t = 0.6 + 0.06(f_c)^{1} \tag{9}$$

Following is the connection between STS and CS for 13 M.

Analysis of Linear Regression

$$f_t = 0.1459 - 1.5944\,(f_{ck}) \tag{10}$$

Analysis of Quadratic Regression

$$f_t = 0.0049(f_{ck})^2 - 0.1482\,(f_{ck}) + 2.7504 \tag{11}$$

Analysis of Cubic Regression

$$f_t = 0.0015(f_{ck})^3 - 0.1265(f_{ck})^2 + 3.7137\,(f_{ck}) - 34.628 \tag{12}$$

The variables are defined as follows: f_{ck} represents the CS in mega pascals (MPa). f_t represents the STS in mega pascals (MPa). Based on the findings, it can be concluded that the linear regression analysis for the 13 Molar 28-day cured GP concretes had satisfactory results. Estimated Split Tensile Strength Values are presented in Table 4. The analysis accounted for 81% (R-Square = 0.8166) of the variability in the STS of the concrete, as measured by cube CS. In terms of cube CS, the quadratic regression analysis explains 83% (R-Square = 0.8311) of the variance in the STS of the concrete, indicating statistical significance as well. When estimating STS in terms of cube CS, this methodology yields satisfactory outcomes since, in most mixtures, the projected values are closer to the actual values than in the case of linear regression evaluation. Concerning cube CS, the cubic regression analysis also fared well in forecasting the concrete's STS. The statistical study demonstrates a substantial relationship, with an R-square value of 0.8444, indicating that 84% of the variance in STS in the concrete can be explained by cube CS. Compared to the other two analyses, this one predicts values rather well for all mixtures. In comparison to the results of the other two analyses, the STS estimated values are found to be rather near to the actual values. As observed from Fig. 20, it was found that compared to linear and cubic analysis, the quadratic model residual analysis presented a more accurate representation of the data.

Test No	Sample No	Pumice (%)	Rubber (%)	Molarity (M)	Compressive strength (MPa)	Split tensile strength (MPa)	Estimated split tensile strength values		
							Linear regression	Quadratic regression	Cubic regression
	GPC_P0_RO	0	0	13	36	3.85	3.66	3.77	5.11
1	GPC1_P5_R0	5%	0%	13	35.1	3.72	3.53	3.59	4.74
2	GPC2_P10_R0	10%	0%	13	33.97	3.23	3.36	3.37	4.35
3	GPC3_P15_R0	15%	0%	13	31.23	3.06	2.96	2.90	3.66
4	GPC4_P5_R5	5%	5%	13	34.41	3.42	3.43	3.45	4.49
5	GPC5_P10_R5	10%	5%	13	33.12	3.02	3.24	3.22	4.10
6	GPC6_P15_R5	15%	5%	13	29.92	2.88	2.77	2.70	3.42
7	GPC7_P5_R10	5%	10%	13	32.18	3.19	3.10	3.06	3.87
8	GPC8_P10_R10	10%	10%	13	31.11	2.55	2.94	2.88	3.64
9	GPC9_P15_R10	15%	10%	13	29.22	2.21	2.67	2.60	3.30
10	GPC10_P5_R15	5%	15%	13	28.46	3.02	2.56	2.50	3.18
11	GPC11_P10_R15	10%	15%	13	26.36	2.22	2.25	2.25	2.84
12	GPC12_P15_R15	15%	15%	13	23.34	1.90	1.81	1.96	2.21

Table 4. STS predictions.

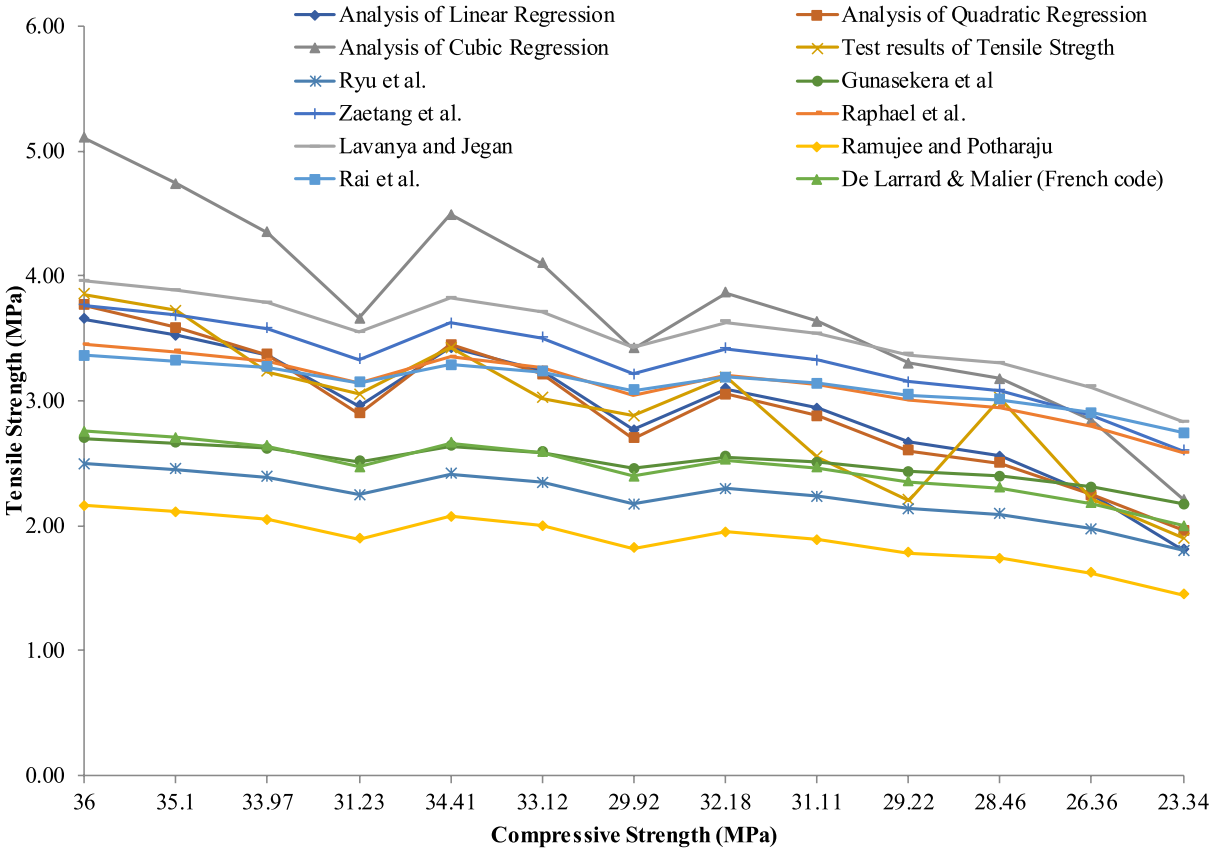


Fig. 20. Compression-STS regression.

Scanning electron microscope (SEM) analysis

SEM analysis was conducted for microstructural examinations. SEM analysis was performed by selecting a piece from the 8th sample. Because in this sample, it was easier to observe when the pumice and rubber ratio was 10% and the strength was at medium levels. Images derived from the SEM analysis are depicted in Fig. 21a–d. Upon examination of these SEM images, it is evident that voids and unreacted FA are distinctly observable. Furthermore, the presence of microcracks, geopolymer gel formation, and notably substantial C–S–H (calcium silicate hydrate) formation is discernible. Specifically, the detailed observation of void formation resulting from the addition of Pumice to the geopolymer mixture is illustrated in Fig. 21a and b. Microstructural analysis in

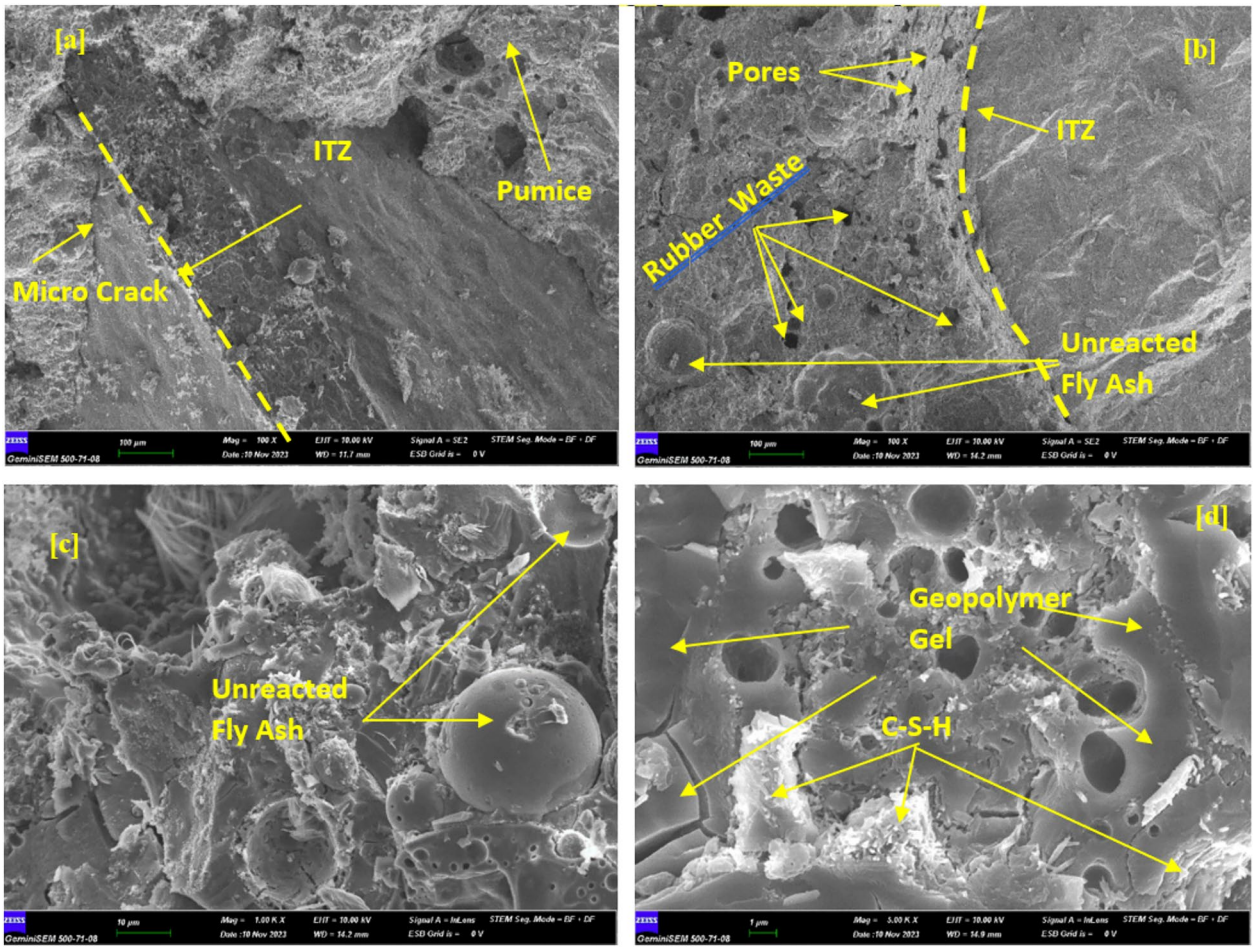


Fig. 21. SEM analysis results.

structural elements is an important issue to observe the distribution and pores of the elements forming the structure by examining the reactions taking place in the internal structure of an element. This analysis is used to understand material properties, determine structural properties, and evaluate material behavior. Additionally, microstructure analysis also plays a critical role in optimizing material processing processes and mechanical properties. In this way, its effects on the durability, performance, and longevity of structural elements can be examined in detail[53–56]. Figure 21a shows the pumice aggregate with large pores in the matrix, while Fig. 21b shows the WTR with a more irregular, rounded shape. Unreacted FA particles are generally spherical or amorphous in structure. Their surfaces are generally smooth and show no traces of dissolution or reactive products, as shown in Fig. 21c[5]. In SEM images, different materials appear with different contrasts. Figure 21d CSH gels are shown; in environments with high calcium content, it may contribute to the formation of CSH gel along with the geopolymerization process. In comparison to other substances that react to generate geopolymer gel, FA substances that do not completely react throughout the alkali activation reaction contribute less and stay weak areas that restrict strength. The concrete's capacity for carrying loads cannot be directly increased by unprocessed FA substances because they do not completely integrate with the matrix; instead, they may cause voids that weaken the concrete[57]. SEM pictures show that the compressive capacity of lightweight concrete may be affected in positive as well as negative ways. The compact, interconnected structure created by geopolymer gel and C–S–H phases improves CS, ensuring persistence under pressure. These phases may contribute to increased levels of strength, since the structure is porous. To maximize strength, however, weak spots like the ITZ region and unreacted particles must be controlled in this kind of lightweight concrete[58].CS may be reduced by several causes, including microcracks, porosity, weaknesses in the ITZ, and unreacted FA particles. It is possible for the load-bearing capacity of the concrete to be reduced due to the presence of voids and loose structures in these different places[59].

It has been observed by a few researchers that there is a clear demarcation between the matrix and the rubber, with the rubber displaying a distinct geometric structure that is more irregular[60,61]. Figure 21b provides evidence in support of these findings. Using morphological analysis, it is possible to quickly identify FA particles that have not yet emitted any reactions. When examined with a SEM, they can be observed as spherical particles that have smooth surfaces. This marks a major surface difference between them and the geopolymer gel that has been reacted. When the clarity and contrast settings are adjusted appropriately, it is possible to distinguish

these particles from other components due to the contrast difference that exists between them and the matrix. It is also possible to utilize energy-dispersive X-ray spectroscopy (EDX), which is included in the SEM apparatus, to verify the chemical composition of the FA particles. It is possible to use EDX to examine these particles since they often include significant concentrations of silica (Si) and aluminum (Al). As an example, the EDX analysis shown in Fig. 22 demonstrates that the particles do, in fact, contain 21.49% silicon and 9.35% aluminum, thus validating their chemical composition.

Energy dispersive X-ray (EDX) analysis

Energy Dispersive X-ray (EDX) analysis is a technique used to determine the chemical composition of a material. This analysis was carried out to understand the components and properties of GPC. In EDX analysis, the electron beam strikes an inner shell of an atom, ejecting an electron and leaving behind a positively charged electron hole. When another electron from an outer shell fills this vacancy, an X-ray is emitted. This analysis works in integration with a SEM. In this way, the EDX analysis applied on the GPC sample shows the presence and density of alumina, silica, calcium, iron, magnesium and other elements in the focused area in the SEM image in Fig. 22. Thanks to the air bubbles formed in GPC concrete containing pumice, Oxygen (O) is seen at the highest rate with 43.15%. Silicon (Si) is an element found abundantly in natural rocks and is seen at a rate of 21.29%. The presence of Si and Al in GPC is a critical factor determining the performance and durability of the material. The silica (SiO_2) present in FA dissolves and becomes active during the alkali activation process. Si dissolves under the influence of alkali activators and transforms into silicate ions. These silicate ions undergo polycondensation reactions with aluminate ions, forming a three-dimensional network structure (geopolymer matrix) composed of Si–O–Si and Si–O–Al bonds. The structure composed of amorphous silica is shown in the SEM image in Fig. 22. This structure provides the mechanical strength and chemical resistance of the concrete. The results are consistent with previous studies[62,63]. In addition to providing information on the distribution of pumice and waste rubber additives throughout the matrix, the elements that were identified in the EDX study highlight the primary components that make up the geopolymer structure. While alkali components like sodium and potassium help the activation and stability of binding structures, the composition's high quantities of oxygen, silicon, and aluminum offer the perfect matrix for the development and endurance of geopolymer gel. With the greatest concentration at 43.15%, oxygen (O) is an important component of other oxide compounds and the structure of the geopolymer gel. In GPC, sodium (Na) and potassium (K) are present at percentages of 15.66% and 2.11%, respectively. These two elements are related to the use of alkali activators. An essential part of the geopolymerization process is played by these alkali elements, which are responsible for activating the Si and Al structures[64]. The geopolymer structure is comprised of essential components such as aluminum (Al) and silicon (Si), with Al accounting for 9.35% and Si accounting for 21.79%, respectively[65]. The presence of these components helps to contribute to the production of geopolymer gel, which in turn helps to enhance the structural strength of anything. The presence of magnesium (Mg) and calcium (Ca) at 1.93% and 2.44%, respectively, often supports reactions within the matrix and contributes to the geopolymer structure. The discarded rubber or pumice may have provided 3.57% of the iron. The concrete has a homogeneous appearance due to a homogeneous matrix of Si–O–Si and Si–O–Al bonding.

TGA analysis

Thermogravimetric Analysis (TGA) is an analysis method that examines the weight change of a material depending on the temperature increase. Thermogravimetric analysis of GPC was performed to determine the thermal behavior and thermal degradation properties of the material. This analysis can help determine how the material responds to temperature change and the separation temperatures of various components. The TGA analysis in Fig. 23 shows the response of GPC concrete with pumice in addition to thermal changes from 0 to 1000 °C. The blue line represents the change in mass. Between 50 and 200 °C, water that is physically bound disappears. The geopolymer matrix's surface or pores evaporate water molecules, causing mass loss. The

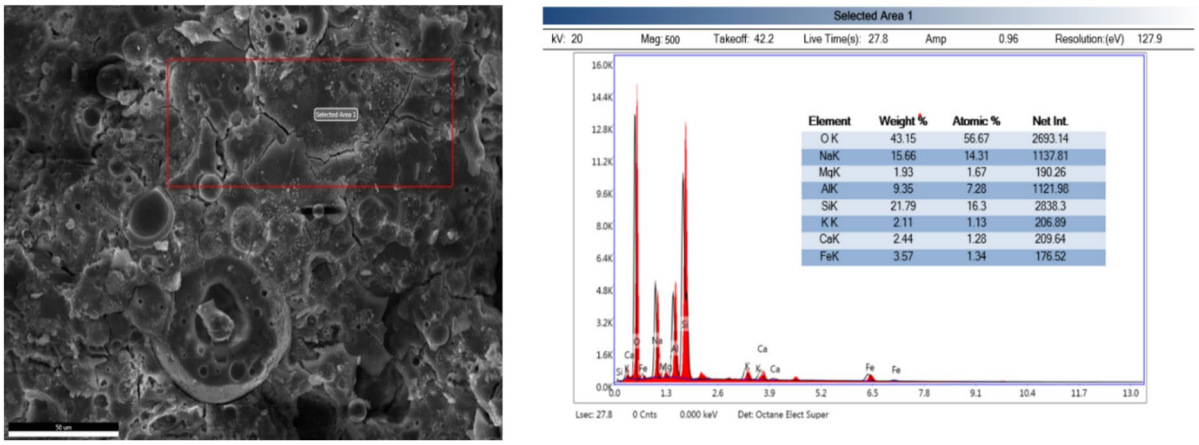


Fig. 22. EDX of the obtained samples.

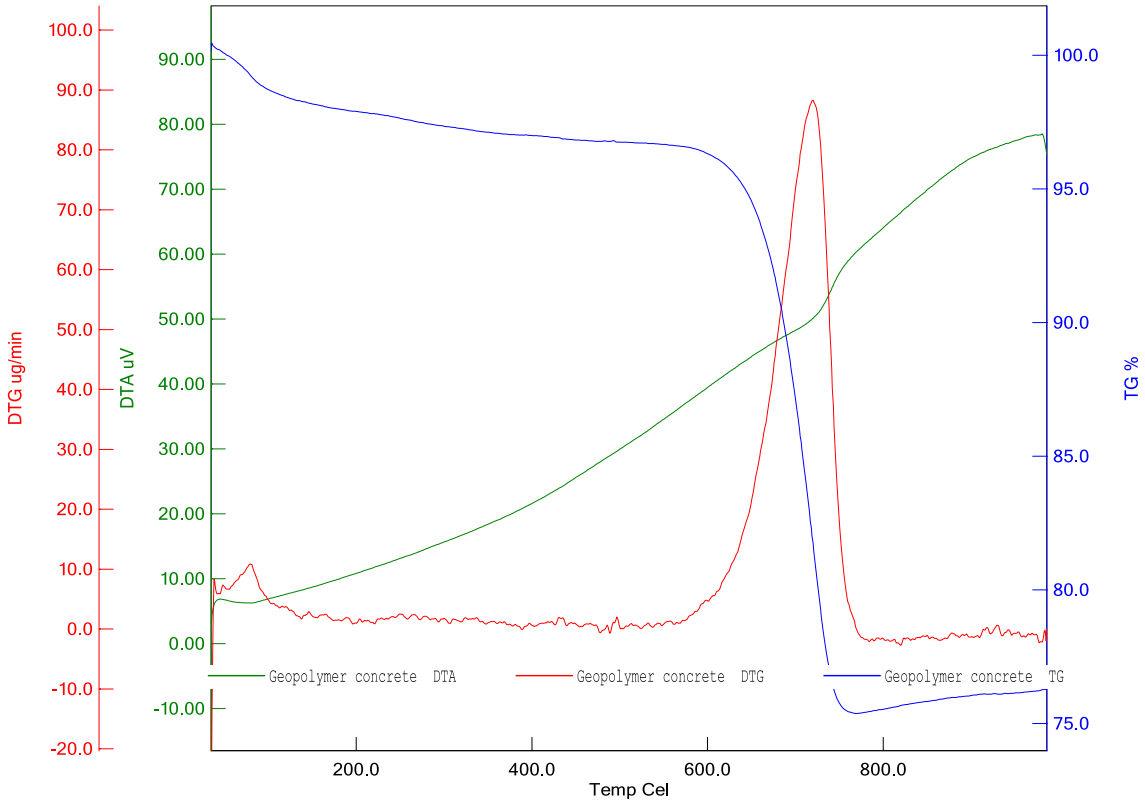


Fig. 23. Thermogravimetric analysis result.

geopolymer structure's chemically attached water molecules break down between 200 and 400 °C. The hydroxyl groups created through the geopolymerization procedure are the source of these water molecules. Geopolymer matrix portions thermally degrade at 400–800 °C. Thermal stress may disrupt Si–O–Si and Si–O–Al bonds, causing mass loss. The geopolymer matrix degrades progressively at 800–1000 °C and higher. Decomposing partially crystalline components and residues increases mass loss. Figure 23illustrates that the original weight was 3.148 mg, and when reaching 1000 °C, it decreased by 76.5%, culminating in a 6% mass loss. Prior research conducted by Aliabdo et al.[66] and Chouksey et al.[67] reported mass reductions of 6–8% and 9–13% of GPC when subjected to temperatures of 800 °C and 900 °C, respectively. Comparing outcomes with less mass loss may be advantageous[66,67]. The green line graph shows DTA analysis findings. This results in the DTA curves peaking. TGA analysis's mass loss profile and temperature ranges may indicate phase transitions. During TGA analysis, as the temperature rises, different components and moisture inside the geopolymer matrix may breakdown or evaporate. These processes may result in phase changes within certain temperature ranges. The peak around 700 °C in the DTA thermogram indicates a phase transition. That is, Si–O–Si and Si–O–Al bonds break under thermal stress, resulting in mass loss. Differential Thermal Analysis (DTG) involves calculating the rate of change of a material's temperature with time. The decomposition of calcium carbonate ($CaCO_3$) into calcium oxide (CaO) typically occurs at this temperature range. If a high-calcium additive, such as ground granulated blast furnace slag, is present, this reaction is expected. This process is associated with the release of CO_2. The statement has been incorporated into the text[68]. It measures how quickly the temperature of the material changes. In this technique, temperature changes that occur when the temperature of a material is systematically increased are documented. In general, it is to reveal the thermal formations or transitions between phases of the material. The DTG result shows the points of lowest and highest temperature fluctuations in the sample as time progresses, as shown by the red line in the diagram[67].

Conclusions

The study explored the combined effects of pumice as a partial replacement of coarse aggregate and WTR as addition in GPC. The mechanical properties, such as CS, STS, and FS, are reduced with increasing replacement levels, but optimum performance can be attained at the lower replacement ratios, especially 5% pumice and 10% WTR. The use of pumice lowers the overall density and enhances sustainability but imparts low strength due to its light weight and porous nature. Likewise, rubberized concrete improves the impact and energy characteristics, thereby making these mixes suitable for shock absorbing and other non-load-bearing uses. Microstructural analysis revealed that the presence of voids and unreacted particles lead to strength reductions, while TGA demonstrated good thermal stability of the geopolymer matrix. The present outcomes emphasize the potential of using the GPC with pumice and WTR as a sustainable material for the aforementioned applications, highlighting the need for further optimization of mix designs for enhanced mechanical performance.

Data availability

Data will be provided upon request from corresponding author (Y.O.Ö).

Received: 18 July 2025; Accepted: 5 September 2025
Published online: 09 October 2025

References

1. Sari, D. & Pasamehmetoglu, A. The effects of gradation and admixture on the pumice lightweight aggregate concrete. *Cem. Concr. Res.* **35**(5), 936–942 (2005).
2. Hossain, K. M. A. Properties of volcanic pumice based cement and lightweight concrete. *Cem. Concr. Res.* **34**(2), 283–291 (2004).
3. Rashad, A. M. A short manual on natural pumice as a lightweight aggregate. *J. Build. Eng.* **25**, 100802 (2019).
4. Ekmen, Ş, Mermerdaş, K. & Algın, Z. Effect of oxide composition and ingredient proportions on the rheological and mechanical properties of geopolymer mortar incorporating pumice aggregate. *J. Build. Eng.* **34**, 101893 (2021).
5. Top, S. & Vapur, H. Effect of basaltic pumice aggregate addition on the material properties of fly ash based lightweight geopolymer concrete. *J. Mol. Struct.* **1163**, 10–17 (2018).
6. Kabay, N. et al. Pumice as precursor in geopolymer paste and mortar. *J. Civ. Eng. Constr.* **10**(4), 225–236 (2021).
7. Safari, Z. et al. Mechanical characteristics of pumice-based geopolymer paste. *Resour. Conserv. Recycl.* **162**, 105055 (2020).
8. Aly, A. M. et al. Performance of geopolymer concrete containing recycled rubber. *Constr. Build. Mater.* **207**, 136–144 (2019).
9. Park, Y. et al. Compressive strength of fly ash-based geopolymer concrete with crumb rubber partially replacing sand. *Constr. Build. Mater.* **118**, 43–51 (2016).
10. Dong, M. et al. Strength and durability of geopolymer concrete with high volume rubber replacement. *Constr. Build. Mater.* **274**, 121783 (2021).
11. Pham, T. M. et al. Dynamic compressive properties of lightweight rubberized geopolymer concrete. *Constr. Build. Mater.* **265**, 120753 (2020).
12. Thomas, B. S. & Gupta, R. C. A comprehensive review on the applications of waste tire rubber in cement concrete. *Renew. Sustain. Energy Rev.* **54**, 1323–1333 (2016).
13. Aslani, F. Mechanical properties of waste tire rubber concrete. *J. Mater. Civ. Eng.* **28**(3), 04015152 (2016).
14. Dheyaaldin, M. H. et al. Sustainable use of waste tire rubbers in eco-friendly and lightweight alkali-activated slag-silica fume mortars. *J. Mater. Civ. Eng.* **36**(12), 04024432 (2024).
15. Mabrouk, A. et al. Effect of curing temperature, silica fume, and waste tire rubber aggregate on material characterization of lightweight geopolymer composite. *Constr. Build. Mater.* **453**, 139063 (2024).
16. Zeyad, A. M. et al. Impact of rice husk ash on physico-mechanical, durability and microstructural features of rubberized lightweight geopolymer composite. *Constr. Build. Mater.* **427**, 136265 (2024).
17. Çoban, Ö. & Akgül, T. Sodyum hidroksit (NaOH) ile aktive edilmiş karo atıklı geopolimer harçların bazı mekanik ve fiziksel özelliklerinin değerlendirilmesi Evaluation of some mechanical and physical properties of sodium hydroxide (NaOH) activated tile waste geopolymer mortars. Pamukkale Üniversitesi Mühendislik Bilimleri Dergisi. **1000**(1000), 0–0.
18. Arioseno, A. D., et al. *Effect of pumice particle treatment on flexural properties of GFRP composite*. In *AIP Conference Proceedings*. (AIP Publishing, 2024)
19. Das, S. & Juneja, D. K. *Improving the performance of porous concrete by utilizing the pumice aggregate*. In *IOP Conference Series: Earth and Environmental Science*. (IOP Publishing, 2024).
20. Karthika, R. B. et al. Experimental study on lightweight concrete using pumice aggregate. *Materials Today: Proceedings* **43**, 1606–1613 (2021).
21. Tanyıldızı, M. & Gökalp, İ. Utilization of pumice as aggregate in the concrete: A state of art. *Constr. Build. Mater.* **377**, 131102 (2023).
22. Çelik, A. İ et al. Study on mechanical, dynamic impact, and microstructural properties of eco-friendly geopolymer paving stones cured in ambient conditions. *Constr. Build. Mater.* **464**, 140132 (2025).
23. Standard, A., *ASTM C349–18: Standard test method for compressive strength of hydraulic-cement mortars (Using Portions of Prisms Broken in Flexure).* Annu B ASTM Stand, 2018: p. 1–4.
24. Astm, C.C.M. *Standard Test Method for Compresive Strength of Hydraulic Cement Mortars (Using 2-in. or 50-mm Cube Sécomens)*. American Society for Testing and Materials Philadelphia, Estados Unidos.
25. Astm, A. *C496/C496M-17 Standard test method for splitting tensile strength of cylindrical concrete specimens*.
26. Oti, J. et al. Mechanical properties of a sustainable low-carbon geopolymer concrete using a pumice-derived sodium silicate solution. *Materials* **17**(8), 1792 (2024).
27. Davidovits, J. *Geopolymer chemistry and applications* (Geopolymer Institute, 2008).
28. Şahan, M. F., Öncel, F. A. & Ünsal, İ. Effect of fiber ratio on the impact behavior of polypropylene fiber reinforced samples. *J. Struct. Eng. Appl. Mech.* **4**(4), 239–248 (2021).
29. Sahan, M. F. & Unsal, I. An experimental analysis for impact behavior of portland cement concrete substituted with reclaimed asphalt pavement aggregate. *Iran. J. Sci. Technol. Trans. Civ. Eng.* **47**(4), 2113–2130 (2023).
30. Öz, H. Ö., Yücel, H. E. & Güneş, M. Bazik pomzanin kendiliğinden yerleşen betonlarin işlenebilirlik özellikleri üzerine etkisi. *Niğde Ömer Halisdemir Üniversitesi Mühendislik Bilimleri Dergisi* **6**(1), 90–97 (2017).
31. Shafiq, M. S. et al. Evaluation of mechanical properties of lightweight concrete with pumice aggregate. *Adv. Sci. Technol. Res. J.* **15**(2), 30–38 (2021).
32. Parhizkar, T., Najimi, M. & Pourkhorshidi, A. R. *Application of pumice aggregate in structural lightweight concrete*. 2012.
33. Yasar, E. et al. Strength properties of lightweight concrete made with basaltic pumice and fly ash. *Mater. Lett.* **57**(15), 2267–2270 (2003).
34. Kurt, M. et al. The effect of pumice powder on the self-compactability of pumice aggregate lightweight concrete. *Constr. Build. Mater.* **103**, 36–46 (2016).
35. Bhavana, N. & Rambabu, C. H. Study of mechanical properties of lightweight aggregate concrete by using pumice stone, ceramic tiles and CLC lightweight bricks. *Int. Res. J. Eng. Technol. (IRJET)* **4**(6), 3071–3079 (2017).
36. Widodo, S., Satyarno, I. & Tudjono, S. Experimental study on the potential use of pumice breccia as coarse aggregate in structural lightweight concrete. *Int. J. Sustain. Constr. Eng. Technol.* **5**(1), 1–8 (2014).
37. Kılıç, A. & Teymen, A. *The effects of scoria and pumice aggregates on the strengths and unit weights of lightweight concrete*. 2009.
38. Rajeswari, S. & George, S. Experimental study of light weight concrete by partial replacement of coarse aggregate using pumice aggregate. *Int. J. Sci. Eng. Res.* **4**(5), 50–53 (2015).
39. Desai, V. B., Arjunappa, K. M. & Sathyam A. An experimental investigation on mode-II fracture of light weight pumice aggregate concrete. *Int. J. Mod. Trends Eng. Res. (IJMER)*, 2014. **4**(12).
40. Sultan, M. A., Gaus, A. & Hakim, R. Review of the flexural strength of lightweight concrete beam using pumice stone as of substitution partial coarse aggregate. *GEOMATE J.* **21**(85), 154–159 (2021).
41. Jalal, M., Nassir, N. & Jalal, H. Waste tire rubber and pozzolans in concrete: A trade-off between cleaner production and mechanical properties in a greener concrete. *J. Clean. Prod.* **238**, 117882 (2019).

42. Manoj, V., Sridhar, R. & Kumar, V. G. A. *Study on effects of pumice in high performance light weight concrete by replacing coarse aggregates* (IOP Publishing, 2021).
43. Reddy, M. S. Y., Rao, V. K. V. & Reddy, M. S. *A study on mechanical and durability properties of structural concrete using pumice and sintered fly ash aggregates* (IOP Publishing, 2021).
44. Sangeetha, S. P. et al. Mechanical characteristics of pumice stone as light weight aggregate in concrete. *Int. J. Sci. Technol. Res* **9**(1), 3760–3762 (2020).
45. Ryu, G. S. et al. The mechanical properties of fly ash-based geopolymer concrete with alkaline activators. *Constr. Build. Mater.* **47**, 409–418 (2013).
46. Gunasekera, C., Setunge, S. & Law, D. W. Correlations between mechanical properties of low-calcium fly ash geopolymer concretes. *J. Mater. Civ. Eng.* **29**(9), 04017111 (2017).
47. Zaetang, Y. et al. Use of coal ash as geopolymer binder and coarse aggregate in pervious concrete. *Constr. Build. Mater.* **96**, 289–295 (2015).
48. Pub, V., *High performance concrete.* 1999.
49. Lavanya, G. & Jegan, J. Evaluation of relationship between split tensile strength and compressive strength for geopolymer concrete of varying grades and molarity. *Int. J. Appl. Eng. Res* **10**(15), 35523–35527 (2015).
50. Ramujee, K. & PothaRaju, M. Mechanical properties of geopolymer concrete composites. *Mater. Today Proc.* **4**(2), 2937–2945 (2017).
51. Rai, B., Roy, L. B. & Rajjak, M. A statistical investigation of different parameters influencing compressive strength of fly ash induced geopolymer concrete. *Struct. Concr.* **19**(5), 1268–1279 (2018).
52. Yan, K. et al. Prediction of splitting tensile strength from cylinder compressive strength of concrete by support vector machine. *Adv. Mater. Sci. Eng.* **2013**(1), 597257 (2013).
53. Çelik, A. İ et al. Mechanical performance of geopolymer concrete with micro silica fume and waste steel lathe scraps. *Case Stud. Constr. Mater.* **19**, e02548 (2023).
54. Ural, N. The significance of scanning electron microscopy (SEM) analysis on the microstructure of improved clay: An overview. *Open Geosci.* **13**(1), 197–218 (2021).
55. Bouaissi, A. et al. Mechanical properties and microstructure analysis of FA-GGBS-HMNS based geopolymer concrete. *Constr. Build. Mater.* **210**, 198–209 (2019).
56. Çelik, A. İ et al. Effect of GBFS ratio and recycled steel tire wire on the mechanical and microstructural properties of geopolymer concrete under ambient and oven curing conditions. *Case Stud. Constr. Mater.* **21**, e03890 (2024).
57. Fernández-Jiménez, A. et al. Mechanical-chemical activation of coal fly ashes: An effective way for recycling and make cementitious materials. *Front. Mater.* **6**, 51 (2019).
58. Alanazi, H. Study of the interfacial transition zone characteristics of geopolymer and conventional concretes. *Gels* **8**(2), 105 (2022).
59. Golewski, G. L. The beneficial effect of the addition of fly ash on reduction of the size of microcracks in the ITZ of concrete composites under dynamic loading. *Energies* **14**(3), 668 (2021).
60. Gupta, T., Sharma, R. K. & Chaudhary, S. Influence of waste tyre fibers on strength, abrasion resistance and carbonation of concrete. *Sci. Iran.* **22**(4), 1481–1489 (2015).
61. Ahmari, S. & Zhang, L. Production of eco-friendly bricks from copper mine tailings through geopolymerization. *Constr. Build. Mater.* **29**, 323–331 (2012).
62. Top, S. et al. Properties of fly ash-based lightweight geopolymer concrete prepared using pumice and expanded perlite as aggregates. *J. Mol. Struct.* **1202**, 127236 (2020).
63. Zeyad, A. M. et al. Production of geopolymer concrete by utilizing volcanic pumice dust. *Case Stud. Constr. Mater.* **16**, e00802 (2022).
64. Provis, J. L. & Van Deventer, J. S. J. *Alkali activated materials: State-of-the-art report, RILEM TC 224-AAM* Vol. 13 (Springer, 2013).
65. Davidovits, J. Geopolymers: inorganic polymeric new materials. *J. Therm. Anal. Calorim.* **37**(8), 1633–1656 (1991).
66. Aliabdo, A. A., Abd Elmoaty, M. & Salem, H. A. Effect of cement addition, solution resting time and curing characteristics on fly ash based geopolymer concrete performance. *Constr. Build. Mater.* **123**, 581–593 (2016).
67. Chouksey, A. et al. An investigation on the effect of curing conditions on the mechanical and microstructural properties of the geopolymer concrete. *Mater. Res. Express* **9**(5), 055003 (2022).
68. Wong, L. S. Durability performance of geopolymer concrete: A review. *Polymers* **14**(5), 868 (2022).

Author contributions

Ali İhsan Çelik: Investigation, Resources, Visualization, Writing—original draft, Conceptualization Memduh Karalar: Investigation, Formal Analysis, Writing—original draft, Writing—review & editing, Ufuk Tunç: Investigation, Writing—original draft, Data Curation Mehmet Fatih Şahan: Investigation, Formal Analysis, Writing—original draft, Data Curation Essam Althaqafi: Writing—original draft, Funding acquisition, Visualization Osman Ahmed Umiye: Writing—original draft, Writing—review & editing, Data curation Yasin Onuralp Özkılıç: Writing—original draft, Writing—review & editing, Data curation, Conceptualization, Methodology.

Funding

The authors are thankful for the financial support provided for this research by the Deanship of Scientific Research at King Khalid University, Abha, Saudi Arabia, through Large Groups RGP2/539/46.

Competing interests

The authors declare no competing interests.

Declaration of generative AI and AI-assisted technologies in the writing process

During the preparation of this work, the authors used ChatGPT in order to improve several important aspects of writing, such as readability, grammar, spelling, and tone of the text. After using this tool, the authors reviewed and edited the content as needed and take full responsibility for the content of the publication.

Additional information

Correspondence and requests for materials should be addressed to O.A.U. or Y.O.Ö.

Reprints and permissions information is available at www.nature.com/reprints.

Publisher's note Springer Nature remains neutral with regard to jurisdictional claims in published maps and institutional affiliations.

Open Access This article is licensed under a Creative Commons Attribution-NonCommercial-NoDerivatives 4.0 International License, which permits any non-commercial use, sharing, distribution and reproduction in any medium or format, as long as you give appropriate credit to the original author(s) and the source, provide a link to the Creative Commons licence, and indicate if you modified the licensed material. You do not have permission under this licence to share adapted material derived from this article or parts of it. The images or other third party material in this article are included in the article's Creative Commons licence, unless indicated otherwise in a credit line to the material. If material is not included in the article's Creative Commons licence and your intended use is not permitted by statutory regulation or exceeds the permitted use, you will need to obtain permission directly from the copyright holder. To view a copy of this licence, visit http://creativecommons.org/licenses/by-nc-nd/4.0/.

© The Author(s) 2025